AD-A138 483 LASER GENERATION OF ULTRASOUND(U) BOLT BERANEK AND NEWMAN INC CAMBRIDGE MA M J RUDD ET AL. FEB 83 BBN-5273 NADC-81067-60 N62269-82-C-0442 1/1

UNCLASSIFIED F/G 14/2 NL

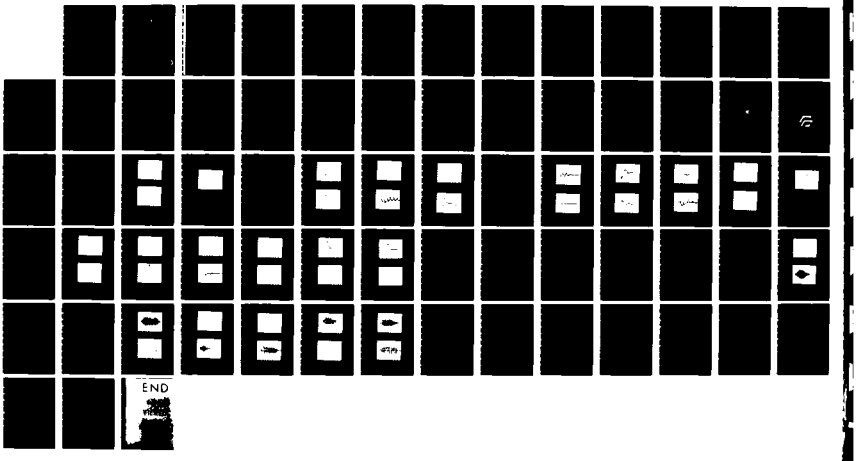

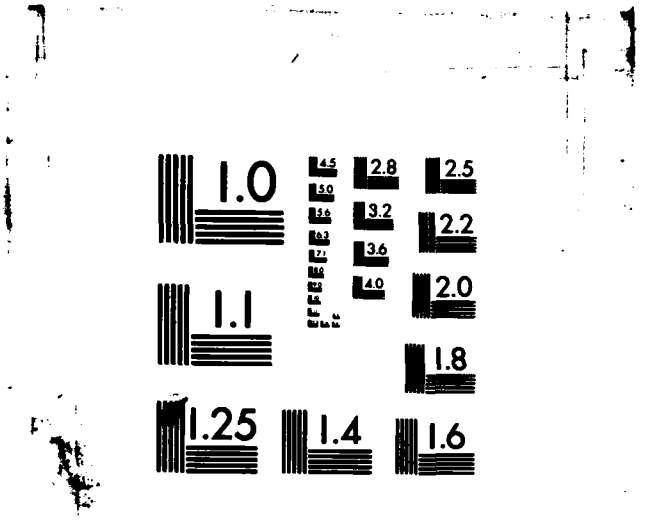

MICROCOPY RESOLUTION TEST CHART
NATIONAL BUREAU OF STANDARDS-1963-A

(12)

REPORT NO. NADC-81067-60

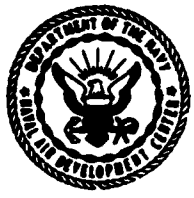

AD A138483

LASER GENERATION OF ULTRASOUND

Michael J. Rudd
Jeffrey A. Doughty

Contract No. N62269-82-C-0442
BBN Job No. 07245

FEBRUARY 1983

Prepared For
NAVAL AIR DEVELOPMENT CENTER
Warminster, PA 18974

Attention: Dr. W. Scott, Code 6063

Prepared By
Bolt Beranek and Newman Inc.
10 Moulton Street
Cambridge, MA 02238

DTIC
ELECTE
MAR 1 1984
S D
B

DISTRIBUTION STATEMENT A
Approved for public release
Distribution Unlimited

FILE COPY

84 03 01 01

NOTICES

REPORT NUMBERING SYSTEM - The numbering of technical project reports issued by the Naval Air Development Center is arranged for specific identification purposes. Each number consists of the Center acronym, the calendar year in which the number was assigned, the sequence number of the report within the specific calendar year, and the official 2-digit correspondence code of the Command Office or the Functional Directorate responsible for the report. For example: Report No. NADC-78015-20 indicates the fifteenth Center report for the year 1978, and prepared by the Systems Directorate. The numerical codes are as follows:

CODE	OFFICE OR DIRECTORATE
00	Commander, Naval Air Development Center
01	Technical Director, Naval Air Development Center
02	Comptroller
10	Directorate Command Projects
20	Systems Directorate
30	Sensors & Avionics Technology Directorate
40	Communication & Navigation Technology Directorate
50	Software Computer Directorate
60	Aircraft & Crew Systems Technology Directorate
70	Planning Assessment Resources
80	Engineering Support Group

PRODUCT ENDORSEMENT - The discussion or instructions concerning commercial products herein do not constitute an endorsement by the Government nor do they convey or imply the license or right to use such products.

UNCLASSIFIED

SECURITY CLASSIFICATION OF THIS PAGE (When Data Entered)

REPORT DOCUMENTATION PAGE		READ INSTRUCTIONS BEFORE COMPLETING FORM
1. REPORT NUMBER NADC-81067-60	2. GOVT ACCESSION NO. A138483	3. RECIPIENT'S CATALOG NUMBER
4. TITLE (and Subtitle) LASER GENERATION OF ULTRASOUND		5. TYPE OF REPORT & PERIOD COVERED FINAL 6. PERFORMING ORG. REPORT NUMBER 5273
7. AUTHOR(s) M.J. RUDD J.A. DOUGHTY		8. CONTRACT OR GRANT NUMBER(s) N62269-82-C-0442
9. PERFORMING ORGANIZATION NAME AND ADDRESS BOLT BERANEK AND NEWMAN INC. 10 MOULTON STREET, CAMBRIDGE, MA 02238		10. PROGRAM ELEMENT, PROJECT, TASK AREA & WORK UNIT NUMBERS
11. CONTROLLING OFFICE NAME AND ADDRESS DR. W. R. SCOTT (CODE 6063) NAVAL AIR DEVELOPMENT CENTER WARMINSTER, PA 18974		12. REPORT DATE February 1983 13. NUMBER OF PAGES 66
14. MONITORING AGENCY NAME & ADDRESS(if different from Controlling Office)		15. SECURITY CLASS. (of this report) Unclassified 15a. DECLASSIFICATION/DOWNGRADING SCHEDULE

16. DISTRIBUTION STATEMENT (of this Report)

APPROVED FOR PUBLIC RELEASE: DISTRIBUTION UNLIMITED

17. DISTRIBUTION STATEMENT (of the abstract entered in Block 20, if different from Report)

18. SUPPLEMENTARY NOTES

19. KEY WORDS (Continue on reverse side if necessary and identify by block number)

Ultrasonics
Lasers
Thermoelastic Waves
Nondestructive Testing

20. ABSTRACT (Continue on reverse side if necessary and identify by block number)

An experimental and analytical study has been conducted into the use of carbon dioxide TEA lasers to generate ultrasonic waves. When the laser is fired at a plastic target, waves with a peak-to-peak pressure of 10 bars are generated. Teflon and Mylar were the most effective. There was no damage to the plastic, even after several hundred shots. This was not the case for glass or aluminum with a much smaller absorption depth and lower conversion efficiency. The sound wave could be directed by using an off-axis zone plate.

DD FORM 1 JAN 73 1473 EDITION OF 1 NOV 65 IS OBSOLETE

UNCLASSIFIED

SECURITY CLASSIFICATION OF THIS PAGE (When Data Entered)

This generated a 10 MHz tone burst, 45° off-axis with a duration of 4 μsec. A theoretical analysis of the phenomena is given which accounts for the waveforms and peak pressures measured.

TABLE OF CONTENTS

DTIC COPY INSPECTED

Accession For	
NTIS GRA&I	☑
DTIC TAB	☐
Unannounced	☐
Justification	
By	
Distribution/	
Availability Codes	
Dist	Avail and/or Special
A-1	

LIST OF FIGURES

LIST OF FIGURES (Continued)

LIST OF FIGURES (Continued)

1. INTRODUCTION

The purpose of this report is to demonstrate a technique to generate high level, focused ultrasound by laser excitation of a material. The application is for ultrasonic nondestructive testing of components and possibly structures.

The principle is that the laser energy is absorbed by a material and heats it, and the resulting thermal expansion generates a pressure wave in the material.

Previous work has been conducted (von Gutfeld 1980) on this technique and the resulting sound wave which was generated was very weak. This report will demonstrate a great enhancement of the mechanism by coating the test specimen with a target material. The target absorbs the laser radiation over a greater depth than the test specimen, typically a metal, and this both increases the efficiency of transduction of the laser energy into sound and also prevents surface damage.

The second phase of the project is to direct and intensify the sound by means of focusing. A holographic lens is used to achieve this focusing. This lens comprises an etched metal zone plate which shades the incident laser beam and focuses the sound.

2. EMPIRICAL MECHANISMS

2.1 Introduction

The use of lasers to induce high-pressure pulses in a solid has been proposed for many years. The applications have primarily been in studying laser damage and for laser weapons. In the current application we wish to avoid such laser damage. This is achieved either by reducing the laser power levels or by applying a protective coating.

The basic mechanism for the generation of sound, which we shall discuss here, is thermo-elastic. The laser heats the surface of the material and causes it to expand. This in turn causes a stress in the material which then propagates as stress waves. In order to achieve sufficiently high resolution for NDT, we require very short pulses, less than 50 nsecs. In order to achieve power in excess of 10 M watts in the short pulse duration, we need a 'Q' switch Neodymium or ruby laser or a carbon dioxide TEA (Transverse Electric Atmospheric) laser. The first two operate in the visible or near infrared and the last in the mid infrared. The TEA laser gives the most power per dollar and operates at a wavelength where many materials, including water, are good absorbers.

Previous work on the use of thermoelastic waves for nondestructive testing was carried out by von Gutfeld (1980). He conducted experiments on flaw detection using a relatively low-power nitrogen laser with a peak power of 100 watts and a duration of 10 nsec. This was focused on the area of about 10^{-4} cm^2 to give peak power of 10^6 watts/cm^2. The total energy in each pulse was only 10^{-6} joules, and much of the acoustic energy was above the bandwidth of the 10-MHz transducer. However, in

spite of his low energy, von Gutfeld was able to identify flaws in test specimens. In later experiments he used a frequency doubled 'Q' switched laser with a peak power of 6 KW, an energy of 0.2 millijoules and a wavelength of 0.532 μm. The laser was frequency doubled from 1.06 to 0.532 μm since more efficient absorption of the laser took place at the latter wavelength. Von Gutfeld focused the laser to a 1-mm diameter spot to give a power density of 10^6 W/cm^2. The acoustic power levels achieved by von Gutfeld were still very low, about 10^{-6} watts. He we shall be looking at techniques to greatly enhance the efficiency of the transduction process.

2.2 Sound Generation by Lasers

A very high-power laser pulse, of the order of 15 megawatts, is fired at a surface and a pressure pulse is generated. There are several mechanisms for generating the pressure pulse and these are discussed below. They are, in order of increasing efficiency,

1) Radiation pressure
2) Ablation
3) Thermo-elastic

2.3 Radiation Pressure

When any electromagnetic wave strikes a surface, there is pressure due to the momentum of the wave. This pressure p is given by

$$p = \frac{W}{c} (1+R) ,$$

where W = power density of the laser pulse, c = speed of light and R = reflectivity of the surface. For a power density of 10^7 watts/cm^2 (10^{11} watts/m^2) c = 3×10^8 m/sec, and R = 0.9, then

$$p = 633 \text{ N/m}^2.$$

The radiated acoustic power S is

$$S = \frac{KA\ p^2}{\rho v},$$

where K = radiation efficiency, A = area of illuminated area, and ρv = acoustic impedance of medium. At high frequencies (above 1 MHz), K ~ 1, A = 5×10^{-4}m^2 and $\rho v = 14 \times 10^6$ rayl for aluminum.

Hence, S = 14×10^{-6} watts.

$$\text{The efficiency} = \frac{S}{WA} = \frac{K}{\rho v} \frac{W}{c^2} (1+R)^2$$

$$= 3 \times 10^{-13}.$$

The efficiency of radiation pressure is extremely low. It is a function of the laser power density W but this cannot be increased much further without the risk of surface damage.

2.4 Ablation

Maccabee, Bell, and Hickman (1980a, 1980b) have proposed and used a CO_2 TEA laser to induce sound in water. The laser radiation, with a wavelength of 10.6 μm, is absorbed in a very

thin (1/2-mil) layer and vaporizes it. The steam so generated is blasted off the surface, and the reaction causes a pressure on the water surface. Very high localized pressures have been achieved in this manner. In addition, work on laser weapons has been looking at methods for generating intense shock waves inside structures using comparable power densities to those discussed here. The model in this case is that some of the metal surface is vaporized and driven off at high velocities, again causing high reaction pressures.

This technique may be applicable to nondestructive testing. For example, a damp tissue might be laid over the metal surface and the water vaporized. The induced pressure

$$p = \frac{W}{L} V_m ,$$

where L = latent heat of vaporization and V_m = ejection velocity, which we will take equal to sound speed in steam. For water, these are 2×10^6 joules/kg and 420 m/sec respectively. Thus

$$p = 2.1 \times 10^{-4} \; W = 2 \times 10^7 \; N/m^2 \text{ for } W = 10^{11} W/m^2.$$

The sound power

$$S = KA \frac{p^2}{\rho v} = KA \frac{W^2 V_m^2}{L^2 \rho v}$$

$$\text{and efficiency} = \frac{S}{WA} = \frac{LWV_m^2}{L^2 \rho v}$$

$$= 3 \times 10^{-4} \text{ for } W = 10^{-11} \text{ watts/m}^2.$$

The efficiency can be increased even further by placing a transparent polyethylene cover over the steam to prevent its escape.

The steam then acts upon the inertia of the cover, increasing the pressure beneath. This will ultimately cause the cover to be "blown" off the surface or else retained by elastic forces around the edge of the cover. This happens on a time scale long compared with the laser pulse.

If very high power levels (10^{11} W/m^2) are incident upon a contaminated aluminum surface, the absorption length can be extremely short (10^{-7} m). Then extremely high temperatures are reached, and the surface layer is not only vaporized but even ionized. The plasma continues to absorb energy and increase its velocity. Velocities of the order of 10,000 m/sec can be obtained. This is 25 times higher than for the steam described above. However, the energy required to heat the plasma is also very much higher than for steam. Reilly, Ballantine, and Woodroffe (1979) have modeled this mechanism, and they predict pressures of about 10^7 N/m for this mechanism for power densities of 10^{11} W/m^2. This is very comparable to the steam ablation predictions. The amount of the aluminum removed is so small (10^{-7} m thick) as to be almost invisible. Thus, although the surface is damaged, the damage is small.

2.5 Theory of Thermoelastic Generation of Ultrasound

2.5.1 Basic mechanism

A laser pulse is fired at an absorbing target. The energy is absorbed in a finite depth in the target. This causes the surface layer to heat up and expand. This causes a volume change in the material and this in turn generates a pressure wave. We shall consider the situation in which the surface area illuminated by the laser is large compared to the wavelengths of the sound involved. Thus the expansion behaves like a piston and generates a plane stress wave. We will ignore the shear stresses involved and just consider a longitudinal acoustic wave. An additional complication arises from the fact that the absorption occurs near a free surface. This causes a much weaker wave to be generated than if the volume change had occurred deep in the medium. There are two ways of seeing this. The first is that because it is easier for the volume to expand in the direction of the free surface it will do so and generate less pressure in the medium. The second view is that the volume expansion generates waves in both directions, propagating both into the medium and towards the surface. On meeting the surface, this latter wave is reflected and inverted. This inverted wave now propagates in the same direction as the original wave. If the two were coincident in time, they would cancel completely because the second wave is inverted relative to the first. However because the inverted wave has had to travel to the surface before it was reflected, it is delayed in time relative to the original wave. Hence the two do not quite cancel and the strength of the resulting wave depends on how far below the surface the source

is. Let us consider a laser pulse of the form

$$W(t) = W\delta(0)$$

where W(t) is the time history of the laser power density and $\delta(0)$ = delta function. Then the temperature distribution T(x) below the surface at a depth x is

$$T(x) = \frac{W\beta}{\rho\sigma}\exp(-\beta x)$$

where

β = absorption coefficient
σ = specific heat
ρ = density of target.

We will ignore thermal diffusion since events take place too rapidly for it to be significant. The volume velocity at depth x is

$$u(x) = \alpha/2 \int T(x)dx$$

where α = thermal expansion coefficient of the target and the 2 because expansion takes place in both directions

$$u(x) = \frac{W\alpha}{2\rho\sigma}\,(1-\exp(-\beta x)) \ .$$

Now we will suppose that the target area is large compared with an acoustic wavelength and that the target behaves like a piston with velocity u. A plane acoustic wave is generated and the pressure p(x) is given by (Kinsler and Frey 1962)

$$p(x) = \rho c\, u(x)$$

$$= \frac{W\alpha c}{2\sigma}\,(1-\exp(-\beta x)) \ .$$

Now the pressure from a plane at a depth x will reach a depth r at a time (r-x)/c later. The pressure to reach a depth r at a time t, originated from a depth r-ct. Thus the direct pressure wave is

$$P_1(r,t) = p(r-ct) \text{ where } ct \leq r$$

$$= \frac{Wac}{2\sigma} (1-\exp-\beta(r-ct) .$$

Now the pressure emanating from the depth x not only propagates forward into the target, but also back to the surface. Here it is reflected and inverted. This arrives at a time (r+x)/c. Conversely the pressure to arrive at a time t has originated from a depth ct-r where ct $\geq$ r. This reflected wave is

$$P_2(r,t) = p(ct-r) \text{ where } ct \geq r$$

$$= - \frac{Wac}{2\sigma} (1-\exp-\beta(ct-r)) .$$

The total pressure is

$$P(r,t) = P_1(r,t) + P_2(r,t)$$

$$= - \frac{Wac}{2\sigma} (\exp-\beta(r-ct)-\exp-\beta(ct-r)$$

where the first term is for ct < r and the second for ct > r. This is the impulse response for the system. The waveform looks like that in Fig. 1 below. The duration of the waveform is of the order $2/\beta c$ where β = absorption coefficient of the medium and c = speed of sound.

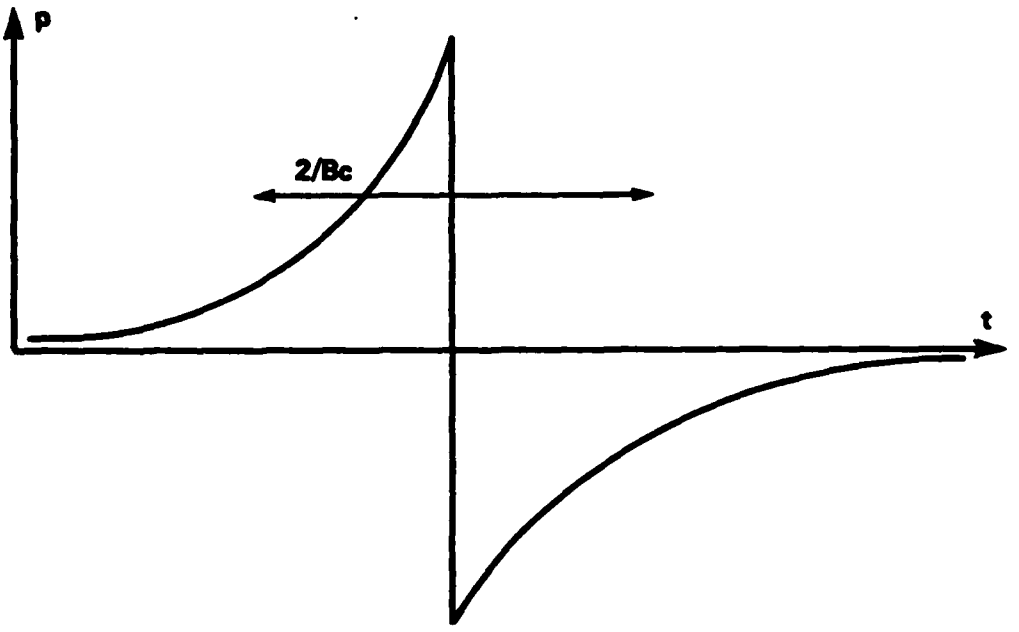

FIG. 1 Waveform from Straightforward Absorption

This is the impulse response of the process. If the laser pulse has a finite duration, then the impulse response is "convolved" with the laser pulse waveform, and the sharp structure of the impulse is "smeared out". If the laser pulse is much longer than $1/\beta c$ then the result is equivalent to differentiating the laser pulse waveform.

2.5.2 Transparent cover

If a transparent cover is placed over the absorber, then it has the effect of increasing the separation between the two halves of the waveform as in Fig. 2 below.

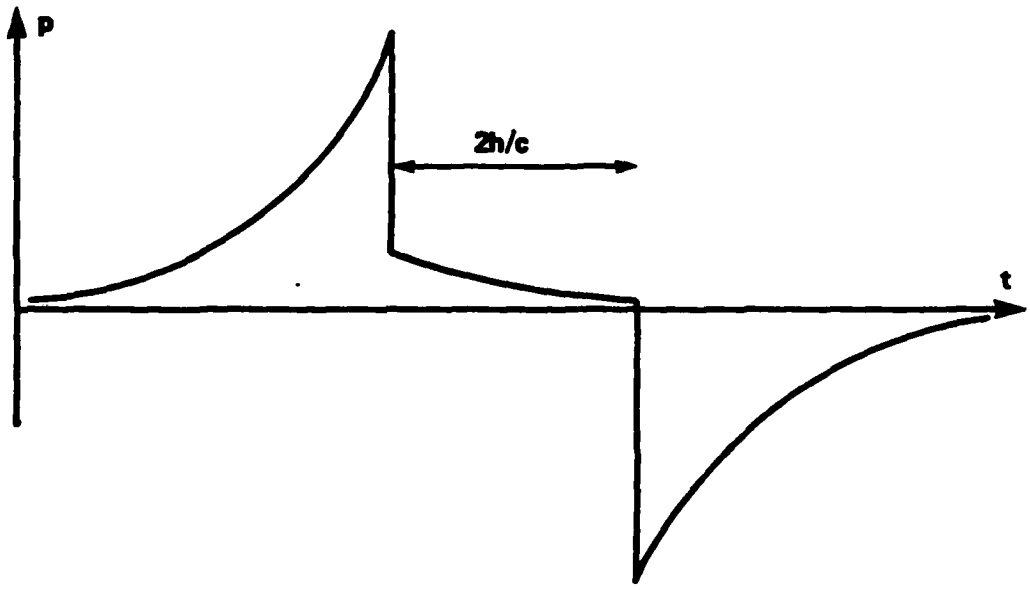

FIG. 2 Waveform Due to Absorption Below a Cover of Thickness L

The typical duration of the signal with this configuration is $2/\beta c + 2h/c$ which is longer than the uncovered case. Thus the cover increases the low frequency energy of the signal.

2.5.3 Examples

Let us consider firing a 50 nsec pulse into water. Water is a very strong absorber with $\beta = 105\ m^{-1}$. Thus the impulse response is only 115 nsec long for a sound speed of 1,500 m/sec. When we convolve a 15 nsec bipolar pulse with a 50 nsec monopolar pulse, the result is small. However, let us suppose we have a cover 80 μm thick with a sound speed of 1,000 m/sec. The delay then is 160 nsec. When this long impulse response is convolved with a 50 nsec pulse then there is little diminution and the result will be an 'N' wave as shown with a duration of 260 nsec as shown in Fig. 3

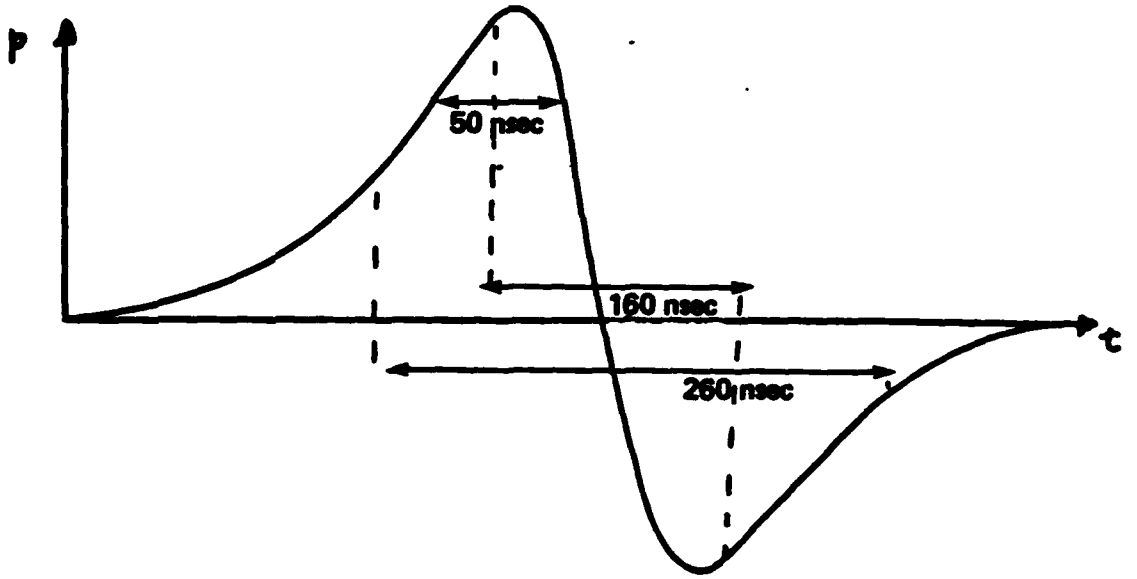

FIG. 3 Waveform for a 50 nsec CO_2 Laser Pulse Fired Into Water Through a 2 mil Window

The peak pressure is

$$P = \frac{c\alpha}{2\sigma} W$$

where W = peak power density of laser = 10^{11} watts/m^2, α = coefficient of thermal expansion of water = 10^{-4}/°C and σ = specific heat = 4×10^3 J/°C/kgm and c = speed of sound = 1,500 m/sec. Thus the radiated sound pressure is 10^6 N/m^2 or 120 bars.

The radiated sound power = $p^2S/\rho c$ where S = illuminated area of target

$$\text{Sound power} = \frac{c\alpha^2 S}{4\rho\sigma^2} W^2$$

$$\text{Efficiency} = \frac{c\alpha^2}{4\rho\sigma^2} W .$$

Note that as long as the laser pulse is shorter than $1/\beta c$, the absorption coefficient β does not enter into the calculation. For many dielectrics and plastics $\beta \approx 10^4$ m^{-1} and c = 10^3 m/sec. Thus the laser pulse must last less than 100 nsec for the model to hold. For metals, β is greater than 2×10^5 m^{-1} and c = 5×10^3 m/sec. The laser pulse must then be less than 1 nsec for the model to be valid.

If the laser pulse is much longer than $1/\beta c$ then the efficiency of transduction is greatly decreased since the generated pressure is the convolution of the impulse response, derived

above, and the laser pulse waveform. This tends to smear out and reduce in amplitude the generated waveform. The result may be thought of as proportional to

$$W(t) - W(t+1/\beta c)$$

where W(t) is the power density of the laser at time t. Thus the resulting pressure is a function of the change in power density over a time $1/\beta c$ or the time differential of the laser power density.

2.6 Laser Damage

The damage done by the laser beam to the surface it is impacting is determined by the temperature rise produced on that surface. Since the laser pulse is so brief, there is no time for thermal diffusion to take place. The heat is then absorbed within the optical absorption depth. The temperature rise ΔT is given by

$$\Delta T = \frac{W\Delta t}{\rho\sigma d} (1-R) \exp(-\beta x)$$

where $W\Delta t$ = laser energy density, $\rho\sigma$ = specific heat per unit volume, d = absorption depth, R = reflection coefficient. For an energy density of 10^4 J/m^2, the temperature rise is 1000°C for aluminum but only 30°C for a plastic, since the absorption depth is much larger.

This is indeed confirmed by experiments. The laser was found to scorch aluminum, but no obvious damage occurred in most plastics.

3. EXPERIMENTAL EQUIPMENT

3.1 Choice of Lasers

For these ultrasonic pressure pulse generation studies we require a laser capable of generating 10 megawatts/cm^2 over an area of at least 1 sq cm so that we can work with a reasonably sized zone plate. The pulse duration must be less than 50 nsec so that there is significant energy up to 10 MHz. There are two types of laser which qualify for this:

(1) 'Q' switched solid state (Neodymium or Ruby)
(2) Carbon dioxide TEA laser.

Three lasers of the first type are listed in Table 1 and one of the second. Nd-glass lasers have been omitted, since the repetition rate of once per minute is considered to be far too slow. Nd-YAG lasers can be fired much more rapidly because of their superior thermal conductivity. It will be noted that the TEA laser not only gives the highest output energy but also has the lowest cost. It also operates at a wavelength where many materials, both aqueous and organic, have very high absorption. Water, for example, has an absorption coefficient of 1000 cm^{-1} at 10.6 μm wavelength, 0.5 cm^{-1} at 1.06 μm and .001 cm^{-1} at .532 μm. Thus it is easy to vaporize 1/2 mil of water in an ablative application. Also it has been found empirically (Avco Research Laboratories) that the grimy aluminum surface typically found on aircraft structures is a reasonable absorber at 10.6 μm. Indeed this is the wavelength being used for high energy laser weapons.

Therefore a carbon dioxide TEA laser was used for this program. It gives the most power for the dollar and operates at a wavelength where there is good absorption, particularly in water.

Type	Manufacturer	Model	Price $K	Wavelength m μm	Energy Joules (TEM_{00})	Pulse Length nsec	Pulse Rate units	Beam Diameter mm
Nd-YAG	General Photonics	Two 46Q	19-23	1.06	.1	10	10-50	6
Nd-YAG (Doubled)	General Photonics	Two 46Q2	20.5-29	.532	.015	8	10-50	6
Ruby	Holobeam	625	27	.649	3 (Multimode)	20	1	13
CO_2 TEA	Tachisto	215A	15	10.6	.5	40	2	6

Table 1 COMPARISON OF LASERS

3.2 Acoustic Apparatus

The acoustic measurements were made in a 10 gallon water tank, with a target for the laser mounted on its wall (see Fig. 4). The CO_2 laser was fired horizontally at the side of the tank without any beamforming optics. This produced an illuminated area of approximately 0.5 sq cm. Three sides of the tank were glass and the fourth was plexiglas, 3/32" thick. The target was either directly on the plexiglas wall or in a window cut in this wall, see Fig. 5.

For the initial measurements, the laser control aperture was fully open so that the laser delivered full power to the target which was only 150 mm away. The laser produced a multimodal beam which tended to vary from shot to shot. Accordingly, for later measurements the aperture was reduced somewhat so that only the TEM_{00} laser mode was produced. This gave a very uniform (gaussian) intensity distribution on the target when it was placed 1.5 meters away. The beampattern was checked using thermally sensitive paper (intended for a thermal printer) which blackened when impacted by the laser beam.

The acoustic pressure in the water tank was measured with a Panametrics V312 immersion transducer with a 10 MHz bandwidth The transducer was 6 mm in diameter. At 10 MHz the acoustic wavelength is 0.15 mm, giving a beamwidth of only 2°, so the transducer had to be aligned very carefully. The transducer was held in a nylon chuck on the end of an aluminum rod. This rod in turn was mounted in an X-Y traverse on the top of the 10 gallon tank. By maneuvering the transducer on this three-dimensional traverse, the acoustic field could be mapped.

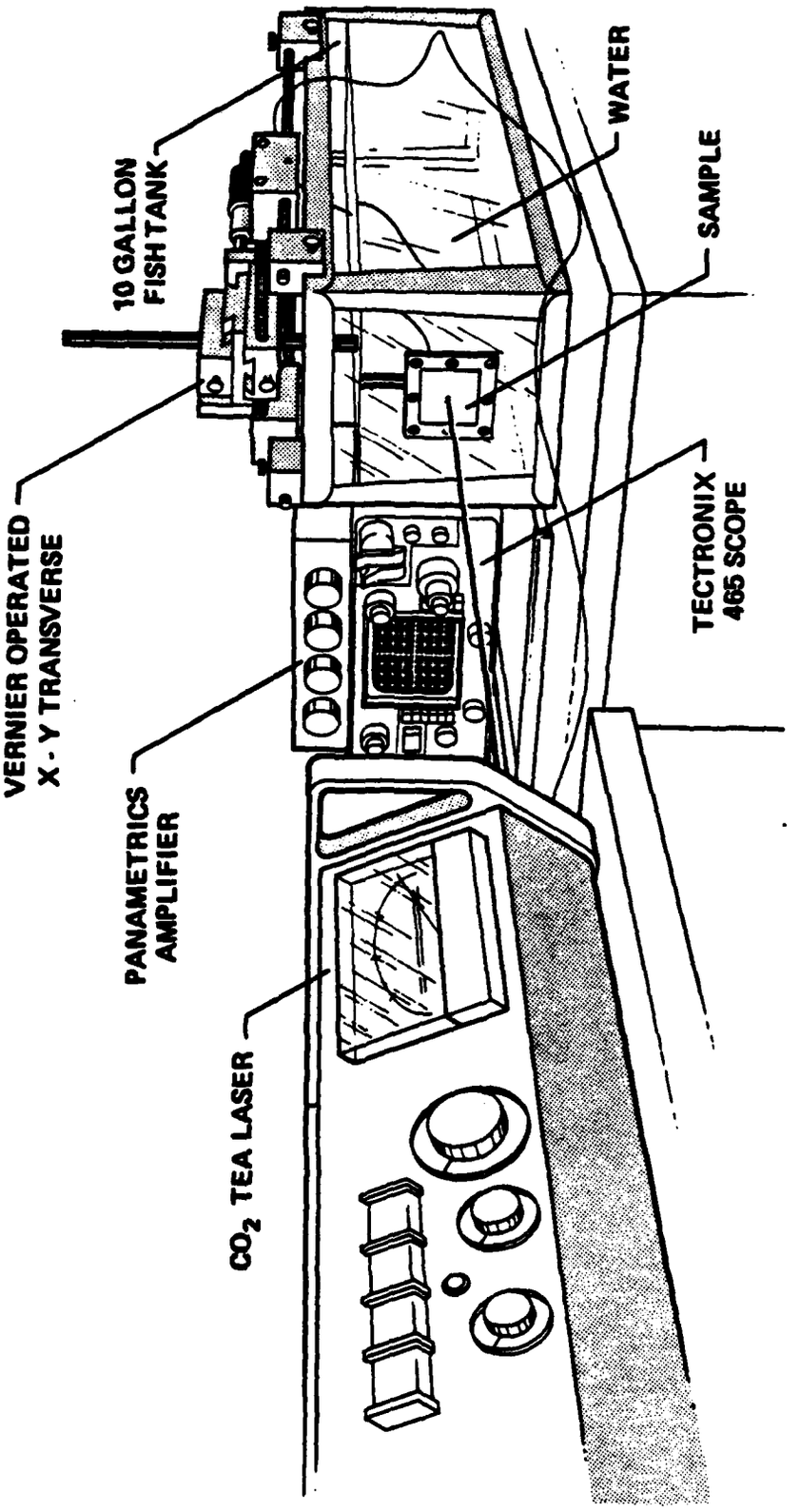

FIG. 4 Overall Test Setup

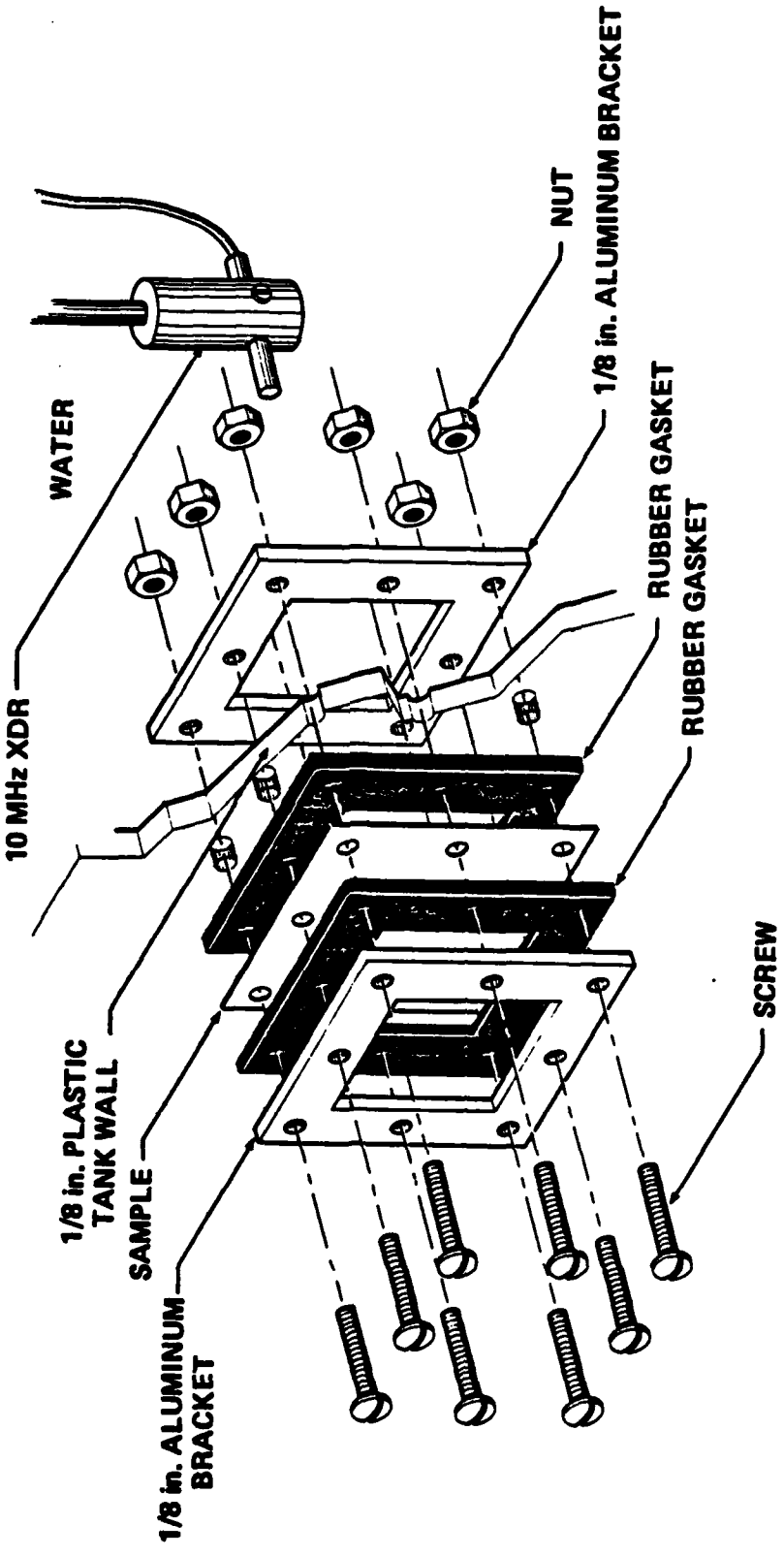

FIG. 5 Arrangement of Samples for Testing

The transducer was calibrated using a reciprocity free field method. The 6 mm diameter transducer was mounted 6 mm in front of a large reflecting plane and pulsed. The magnitude of the reflection was measured, together with the drive voltage. The reciprocity relation for a plane wave transmitter to a plane wave receiver was used. For a large piston transducer close to the reflector, the sensitivity in volts per pascal is given by (Beranek 1954):

$$\left[\frac{Re_2 \pi a^2}{e_1 \rho c}\right]^{\frac{1}{2}}$$

where:

R = electrical impedance of transducer, at operating frequency

e_1 = voltage input to the transducer, creating acoustic field

e_2 = voltage output from transducer, caused by acoustic field

a = radius of transducer

ρc = characteristic impedance of water = 1.5×10^6 rayls.

In this method, voltage was supplied to the transducer, creating a sound field. The sound would travel out, hit the reverberant tank side and return to the transducer where it would be sensed and an output voltage obtained. The test was conducted using a Panametrics transmitter/receiver. It supplied a 100 volt pulse to the transducer then received the output and transferred it to a Tektronix oscilloscope. An output of 4.6 volts was recorded for a transducer of radius 3 mm and impedance of 30 ohms. Using the above equation, this corresponds to a sensitivity of -106 dB re 1v/pascal or -126 dB re 1v/μbar. This is a sensitivity of 0.5 volts/bar.

4. TESTING, PHASE I

The first phase of testing was to determine the feasibility of using plastic to produce measurable acoustic levels in the tank. To begin with, the laser was fired at the plexiglas side of the tank. When the transducer was positioned so as to maximize the signal a two volt peak to peak "N" wave with a duration of 500 nsec was produced (see Fig. 6). This corresponds to a peak pressure of approximately 2 bars.

The test was conducted with the laser in its full open position, about 6 inches from the tank surface. In this case it would be delivering the full 15 megawatts over a surface of about 10 by 20 mm for a power density of 1.25×10^{11} W/m . It is worth noting that at this power density the surface of the plexiglas, as with many materials tested, displayed no surface damage.

The next step was to test a different plastic, Homolite 911. The target was plated on the outside of the plexiglas. A 1/16 inch thick piece 2 inches square was coupled to the plastic side of the tank by means of petroleum jelly. The laser, under the same conditions as the previous test, was fired at the plastic. It produced the 1.4 V p-p "N" wave shown in Fig. 7. The period is about 450 nsec.

In order to determine how much of the signal was coming from thermoelastic mechanisms and how much, if any, was occurring by ablation, the 911 sample was covered with Scotch tape. The tape is polyethylene which has a very low IR absorption. If ablation occurred, the polyethylene tape would over the duration of the laser pulse restrict the released gas, creating more pressure and increasing the acoustic signal. In this case the output decreased to about .6 V_{p-p} and the period was the same at 450 nsec. This is shown in Fig. 8. Therefore, for 911, surface ablation probably does not exist.

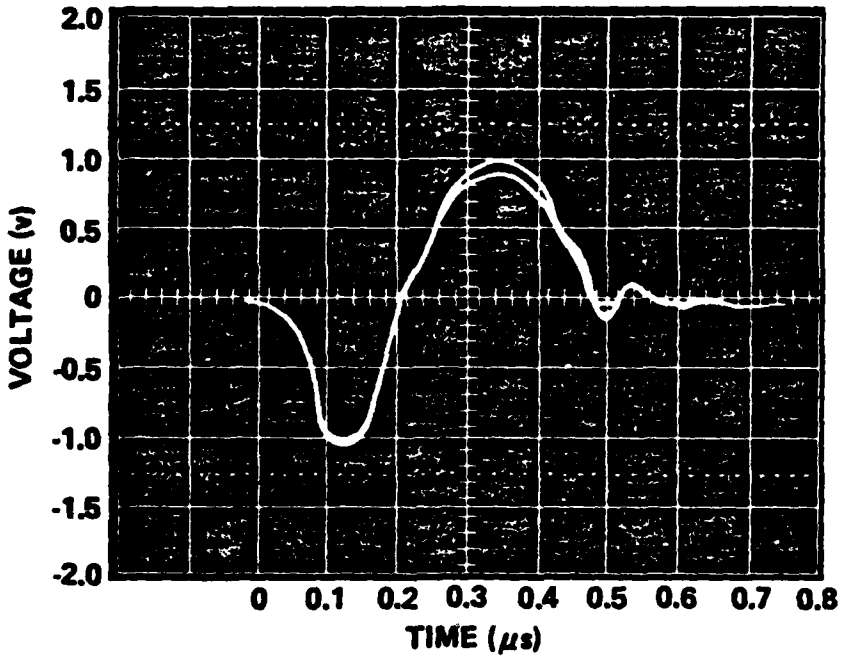

FIG. 6 Plastic Side of Tank Only

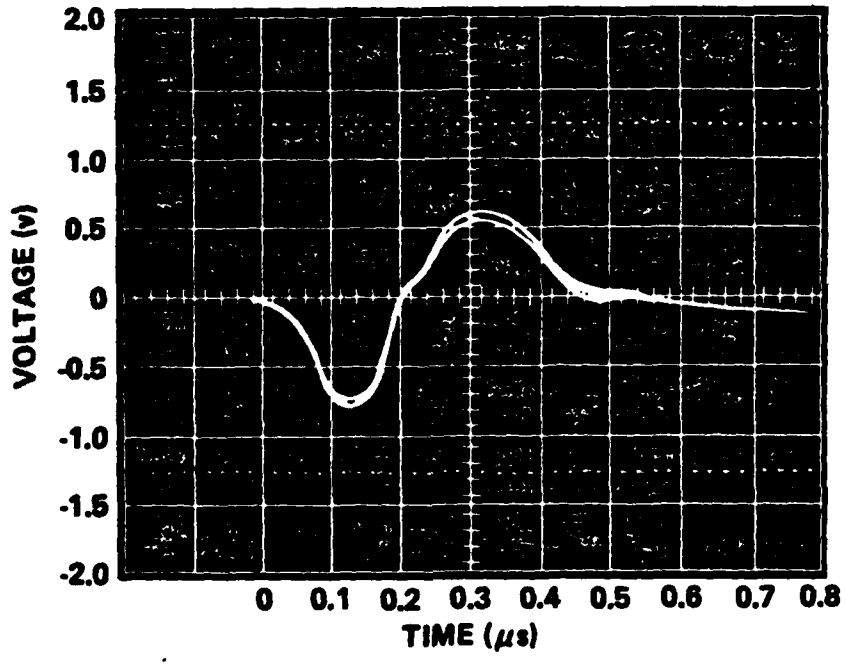

FIG. 7 1/16" Homolite 911 on Tank

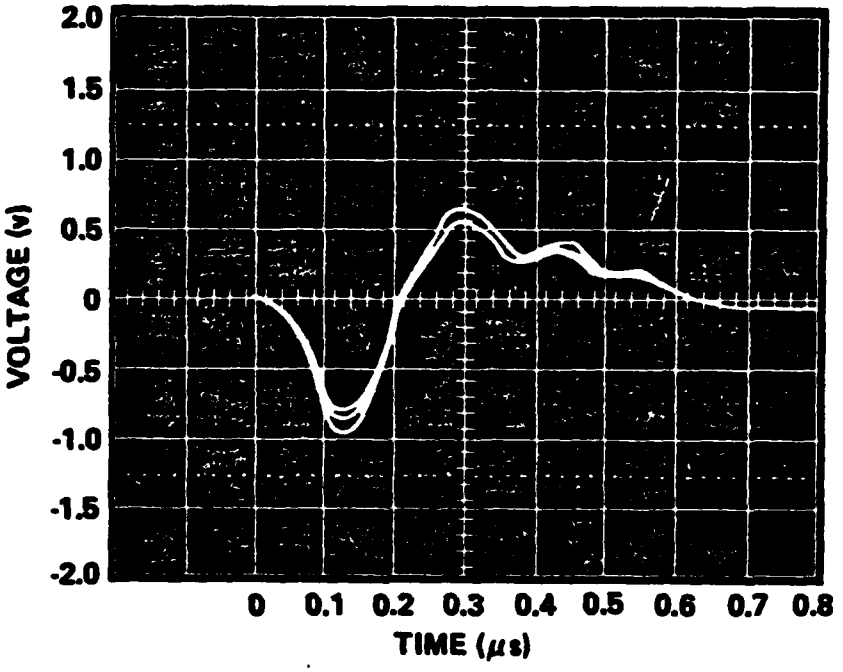

FIG. 8 1/16" 911 on Tank With Scotch Tape

The glass was also tested (see Fig. 9). It produced a .075 v_{p-p} signal at about 150 nsec. However, due to its high absorption, very high temperatures are reached at the surface of the glass. Thus after about 50 shots, the glass was noticed to have severe surface etching.

The following tests were conducted on various materials to determine their proficiency of transduction. All tests were conducted in a similar manner to the Homalite 911 test; at close range, the full open laser aperture, and with similar specimen thicknesses. They were conducted so that the "best" material could be determined and tested further.

PLEXIGLAS (Fig. 10): A 1/8 inch thick plexiglas sample was tested. An output level of .225 v_{p-p} and a duration of 550 nsec were recorded.

ACRYLITE (Fig. 11): A 1/8 inch thick sample of red acrylite was tested. A 450 nsec, .35 v_{p-p} signal was recorded.

NYLON (Fig. 12): An 1/8 inch thick sample of white nylon was tested. A signal of .12 v_{p-p} and only 3.1 μsec period was noted. The waves may be related to reverberation within the material.

POLYETHYLENE (Fig. 13): A piece of 10 mil polyethylene sheet was placed over the plastic side of the tank. This produced a signal of .8v at 800 nsec. The sheet began to melt after about 30 shots.

PAPER PHENOLIC (Fig. 14): A 1/16 inch thick piece of paper phenolic was tested and produced a .225 v_{p-p}, 475 nsec signal.

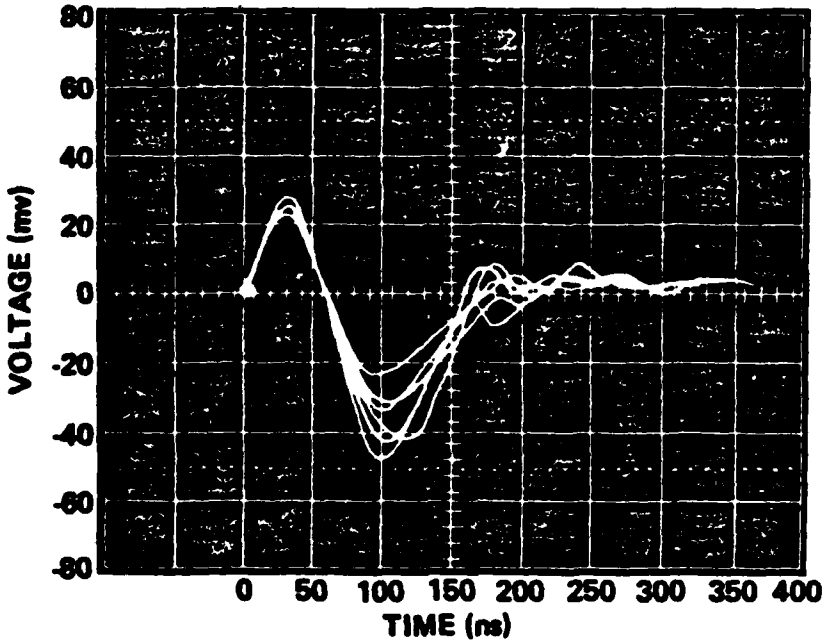

FIG. 9 Glass Tank Side

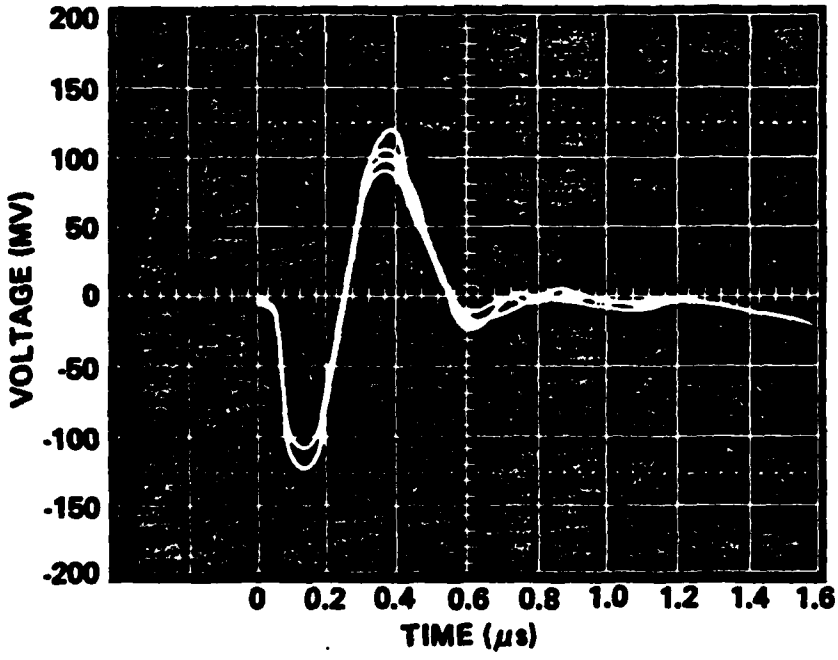

FIG. 10 Plexiglas Sample on Tank

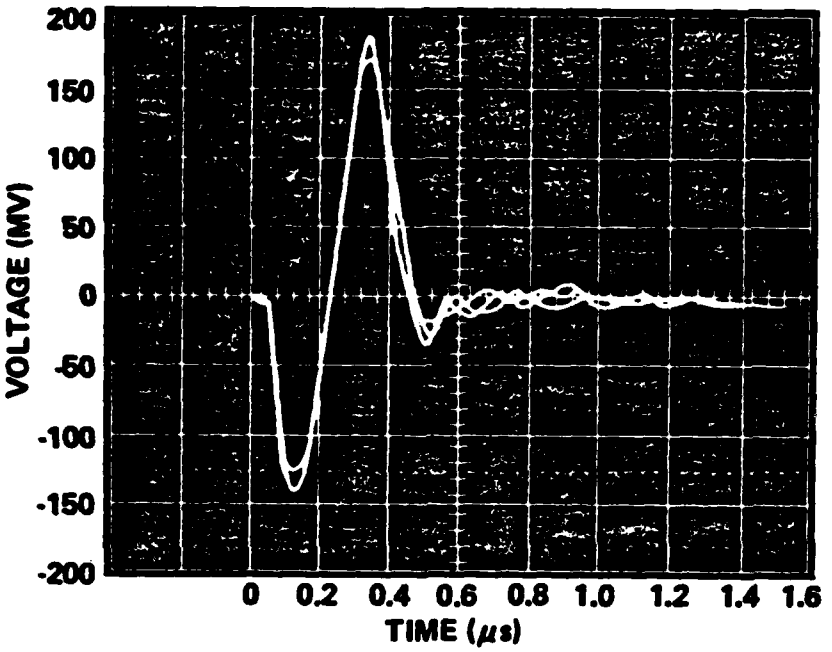

FIG. 11 Acrylite on Plexiglas

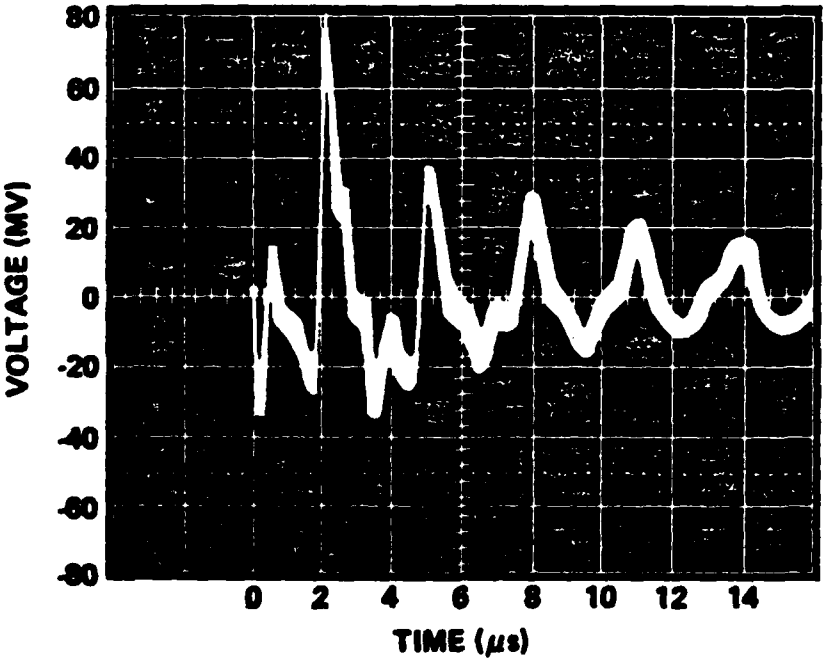

FIG. 12 Nylon Sample on Tank

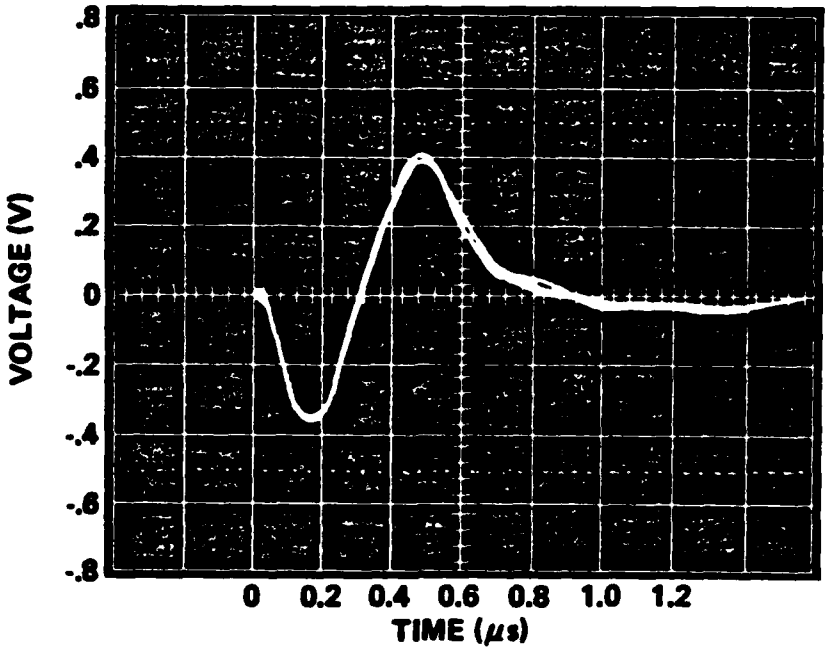

FIG. 13 Polyethylene Sample on Tank

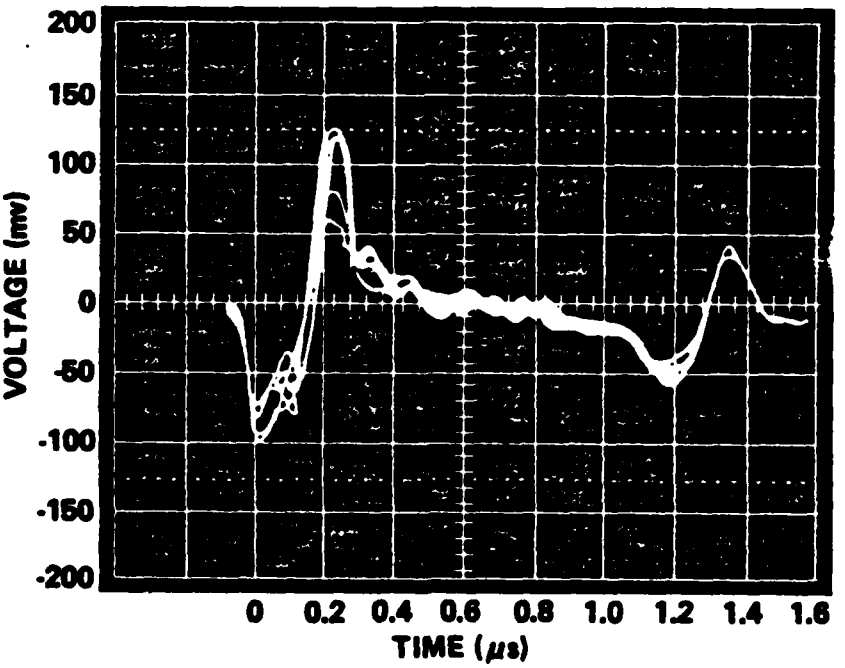

FIG. 14 Paper Phenolic on Tank

POLYPROPYLENE (Fig. 15): A 1/32 inch thick piece of polypropylene was tested. It produced a 1 v_{p-p}, 1,400 nsec signal.

G11 EPOXY (Fig. 16): A G11 sample 1/16 inch thick produced a .175 v_{p-p}, 240 nsec signal. During testing, darkening of the epoxy filler was noticed, probably due to heating.

DELRIN (Fig. 17): A 3/32 inch thick sample of Delrin was tested. It produced a .4 v_{p-p}, 1750 nsec signal. However, a large acoustic signal in the air was produced due to surface ablation and/or extreme outgassing. A very loud crack and a puff of smoke, accompanied by flame, was noted. Surface damage in the form of indentations was observed.

FABRIC PHENOLIC (Fig. 18). A 1/32 thick sample of fabric phenolic was shown to produce a .3 v_{p-p}, 500 nsec signal.

G10 EPOXY (Fig. 19): A G10 epoxy sample, 1/8 inch thick was tested. It produced a signal of .09 v_{p-p} and 270 nsec.

HIGH DENSITY POLYPROPYLENE (Fig. 20). A 3/16 sample of High Density Polypropylene was tested. It produced a signal of .35 v_{p-p} and 2,000 nsec.

KAPTON (Fig. 21): A sheet of 2 mil Kaptan was tested. It displayed a 2 v_{p-p}, 575 nsec response.

PVF2 (Fig. 22). Four mil PVF2 sheet was then tested. It produced a 2.5 v_{p-p}, 560 nsec signal.

METALLIZED PVF2 (Fig. 23): Thin metallized PVF2 film was tested. The response in Fig. 20 is after the metal is ablated away. This signal is 2.1 v_{p-p} at 600 nsec. Before the metal ablated and during its ablation, the signal produced was lower. The metallized side of the plastic was toward the laser.

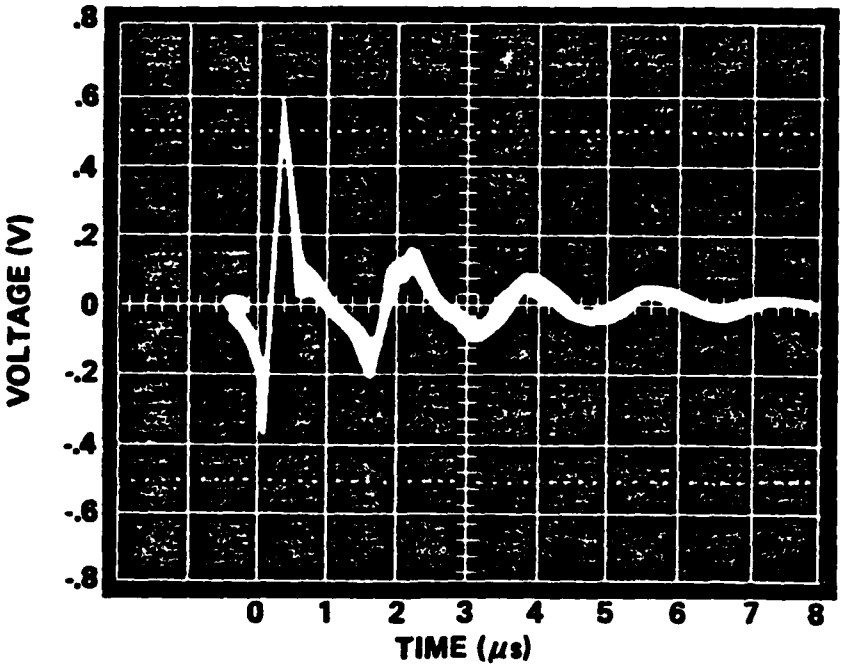

FIG. 15 Polypropylene Sample on Tank

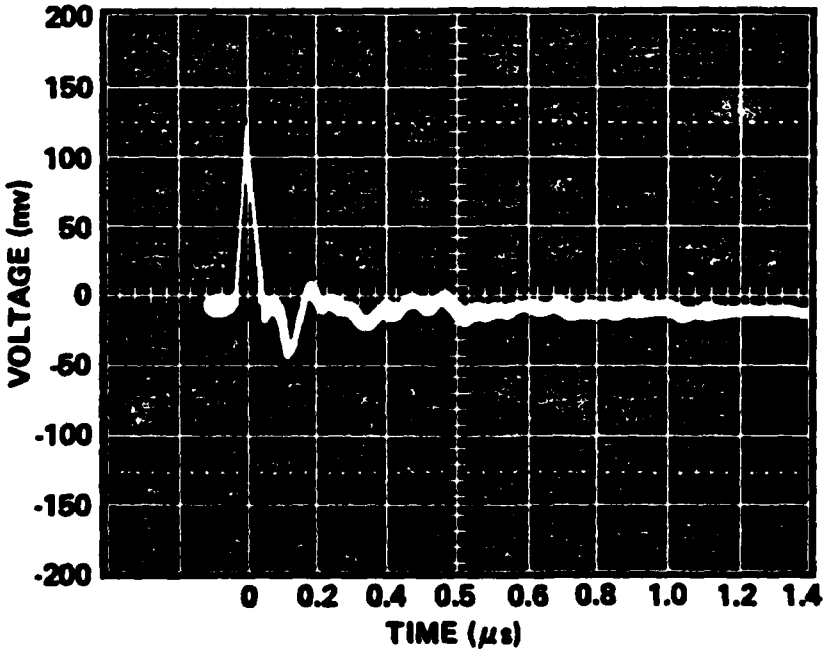

FIG. 16 G11 Epoxy Sample on Tank

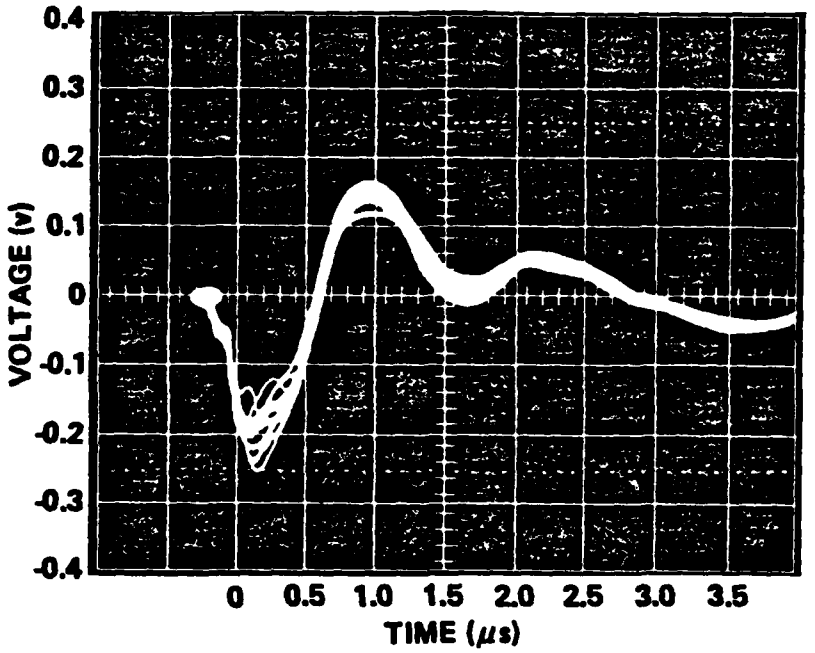

FIG. 17. Delrin Sample on Tank

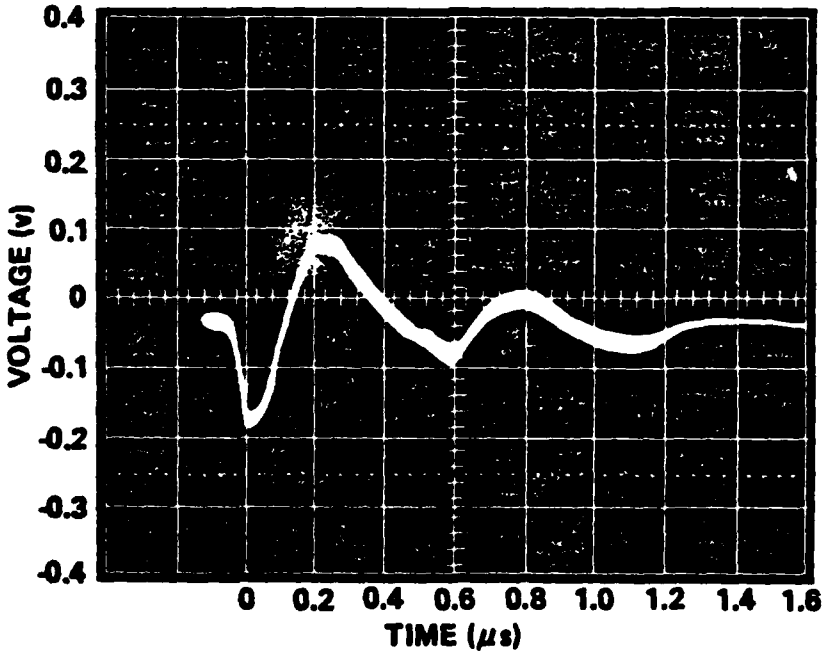

FIG. 18 Fabric Phenolic on Tank

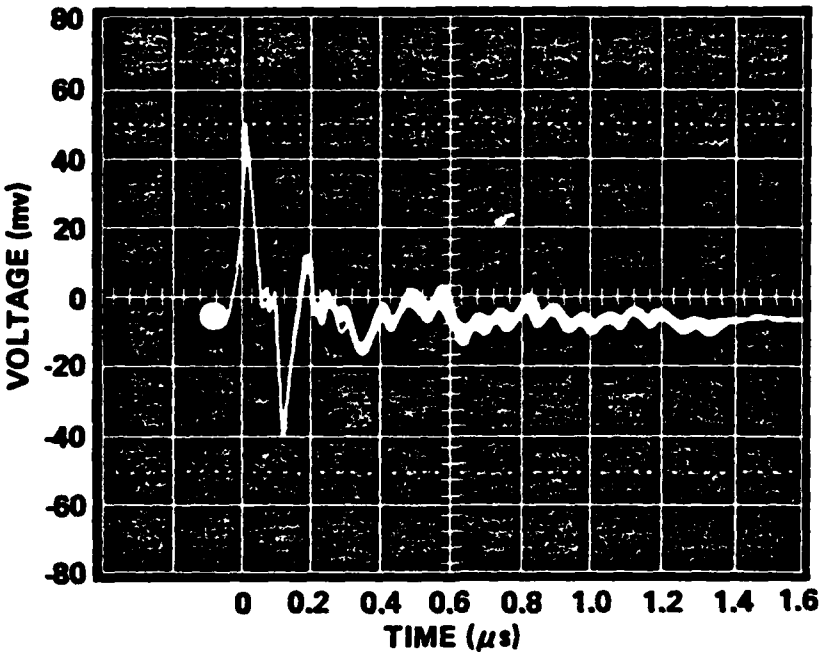

FIG. 19 G10 Epoxy Sample on Tank

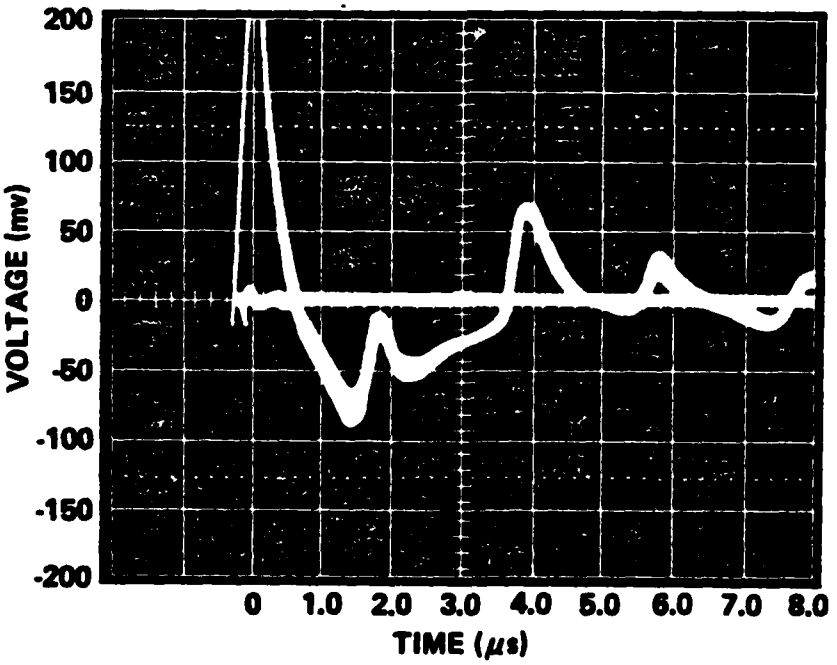

FIG. 20 High Density Polypropylene Sample on Tank

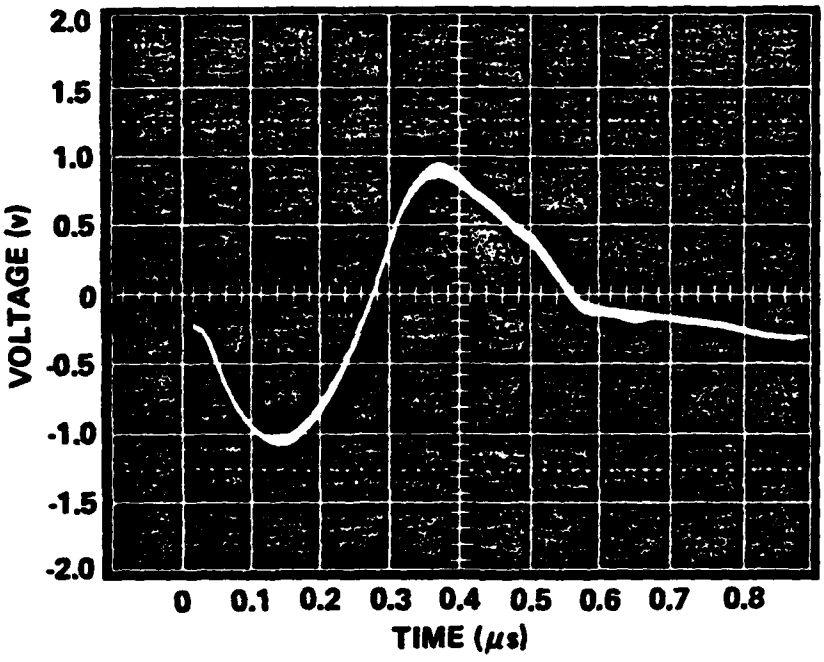

FIG. 21 4mil Kapton Sample on Tank

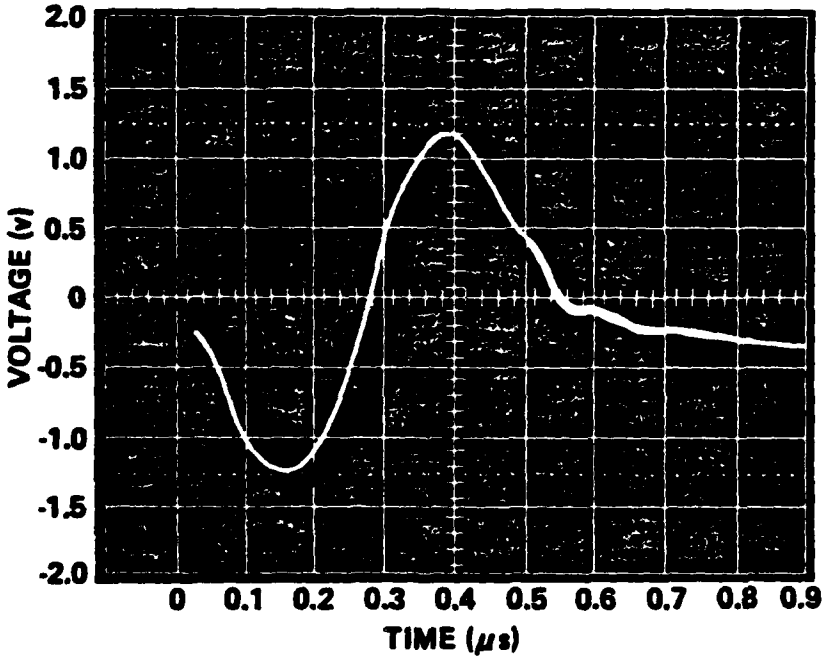

FIG. 22 PVF2 Sample on Tank

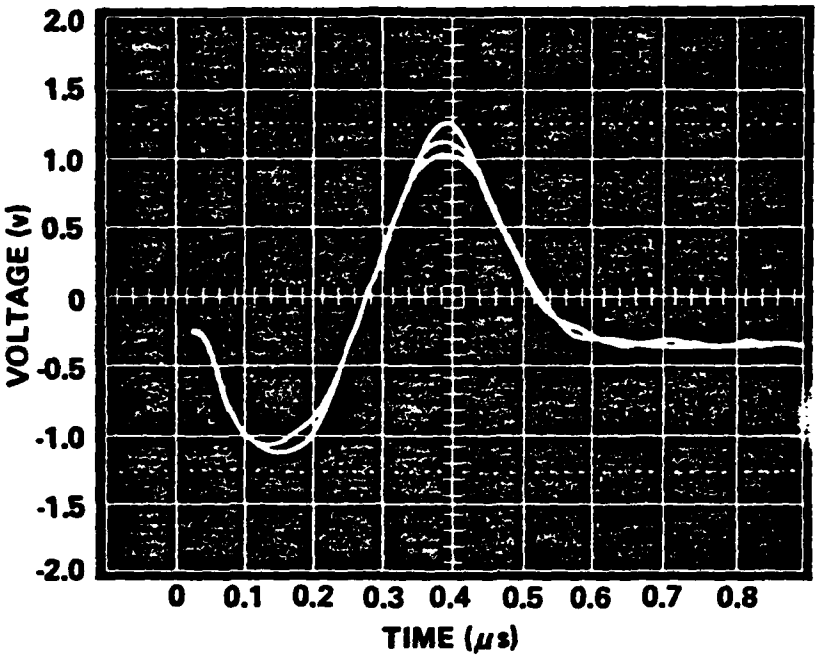

FIG. 23 Metalized PVF2 Sample

TISSUE WITH WATER (Fig. 24): To test the effects of ablation, a Kleenex tissue was soaked with water and stuck to the side of the tank. The laser was fired and steam was noticed, producing a .5 v_{p-p}, 400 nsec signal. The signal was much less reproducible than that of the thermoelastic tests.

TEFLON (Figs. 25 to 29). Figures 25 through 28 show the response of four different varieties of Teflon. All are 2 mil sheets and all have a response of 3 v_{p-p} and 800 nsec. Figure 29 shows the response of a 1/16 inch thick sample of an unknown variety probably TFC due to its off-white color) of Teflon. It too produces a signal of about 3 v_{p-p} but the duration is slightly longer at 1,000 nsec. This test shows that the added thickness of Teflon did not attenuate the amplitude of the signal.

MYLAR (Figs. 30 to 35). The figures show the results of testing on a variety of Mylar samples. The thicknesses are 1/2, 2, 3, 4, 5 and 7 mils respectively. They produce slightly more output than do the Teflon except for the 1/2 and 2 mil ones where it is believed that much of the IR energy goes through the sample to the water, exciting it rather than the material. The thicker samples average about 4 volts peak to peak at around 2.5 MHz.

It should be noted that the 2 and 4 mil samples (Figs. 31 and 33) survived only 20 to 30 shots from the laser before melting. In order to test these samples, 1/2 mil sheet was placed over it and pressed firmly. With this in place, the samples resisted melting long enough so that measurements were taken, some sign of melting was observed, however, it was much less than it was in the initial case.

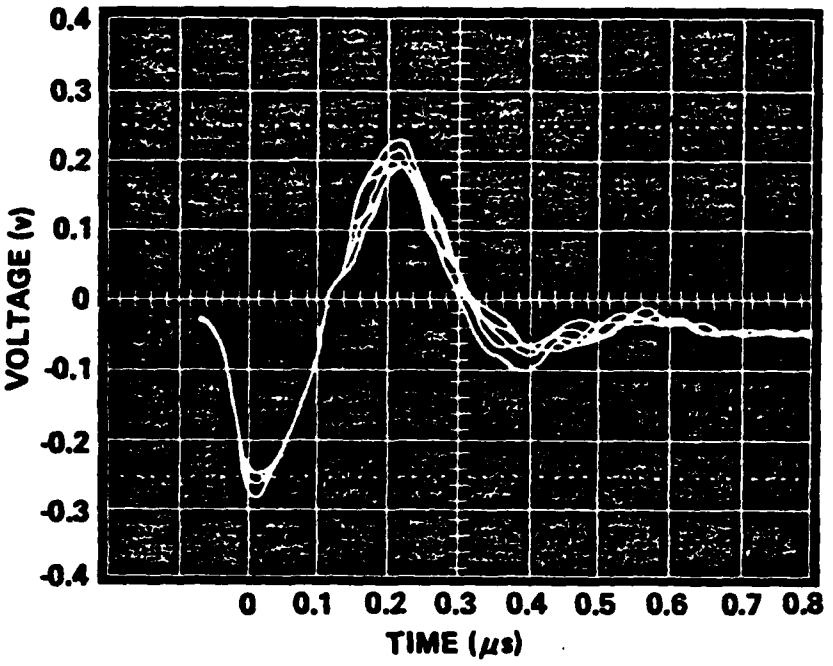

FIG. 24 Tissue Soaked in Water on Tank

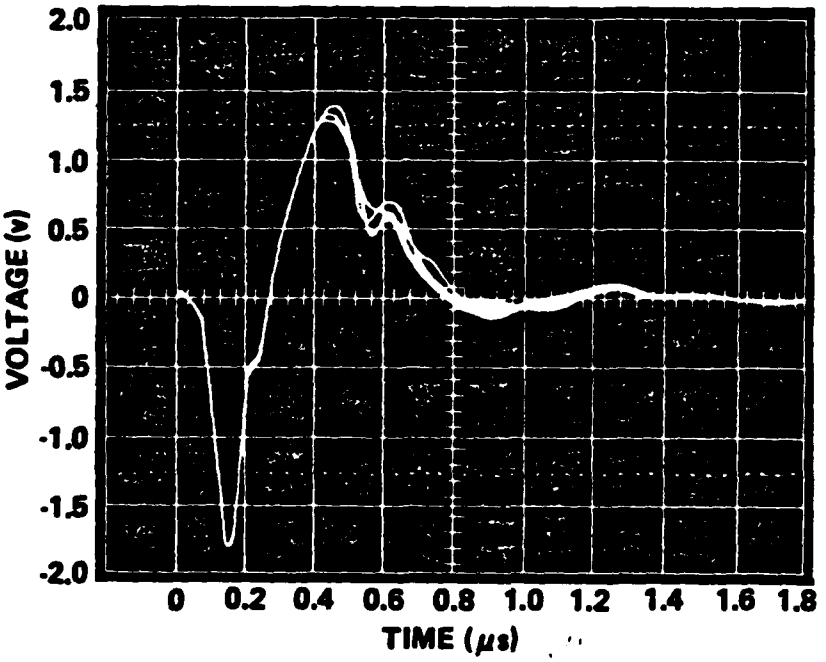

FIG. 25 2mil Teflon TFE Sample on Tank

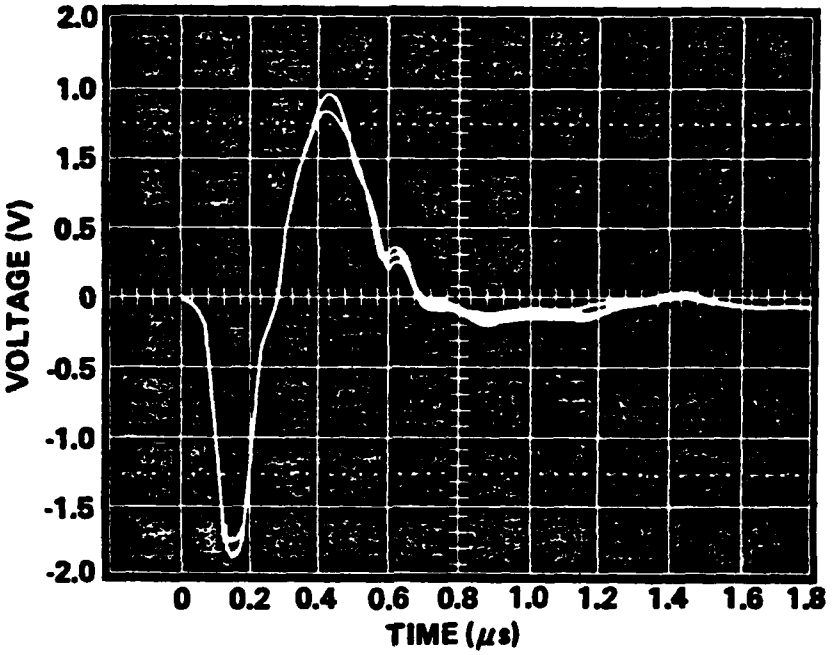

FIG. 26 2 mil Teflon PFA Sample on Tank

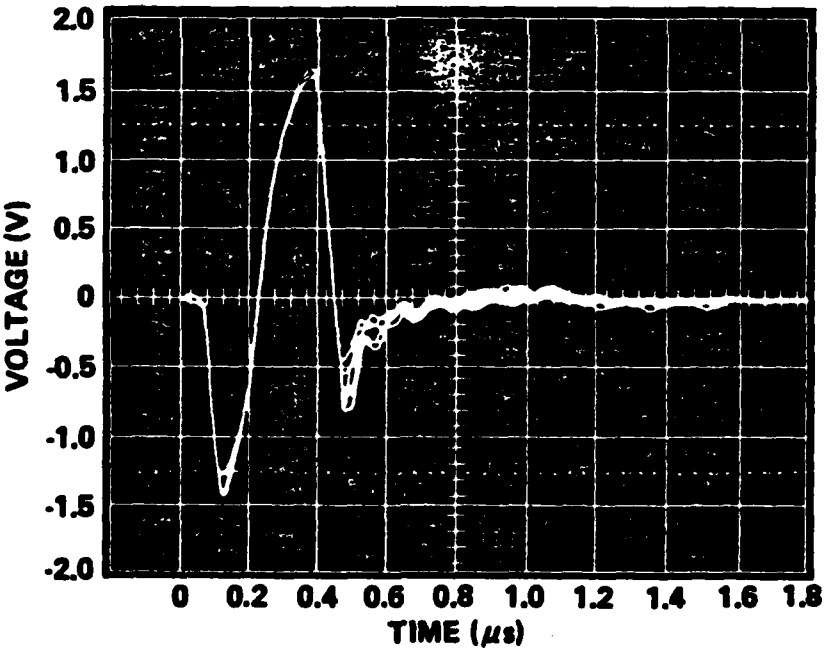

FIG. 27 2 mil Tefzel Sample on Tank

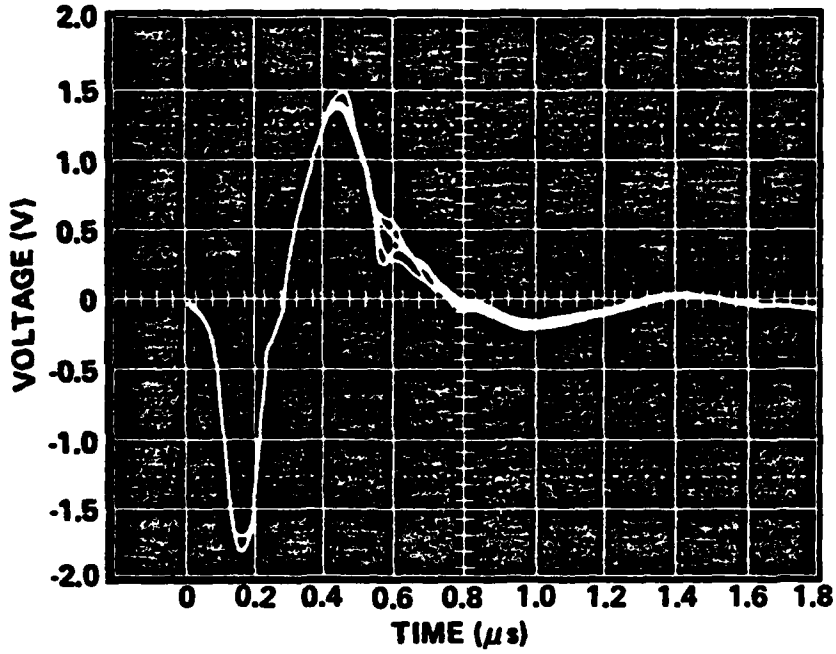

FIG. 28 2 mil Teflon FEP Sample on Tank

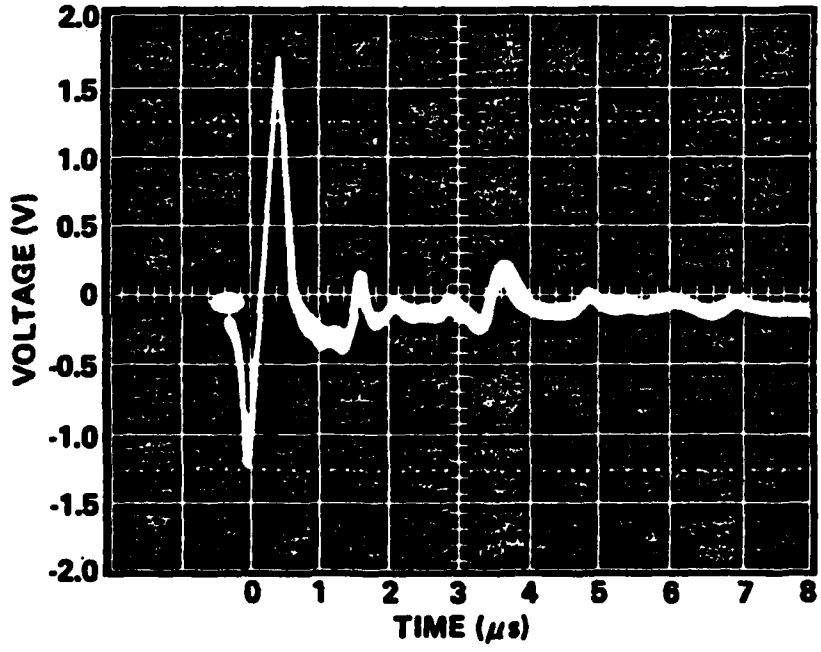

FIG. 29 Unidentified Teflon Sample on Tank

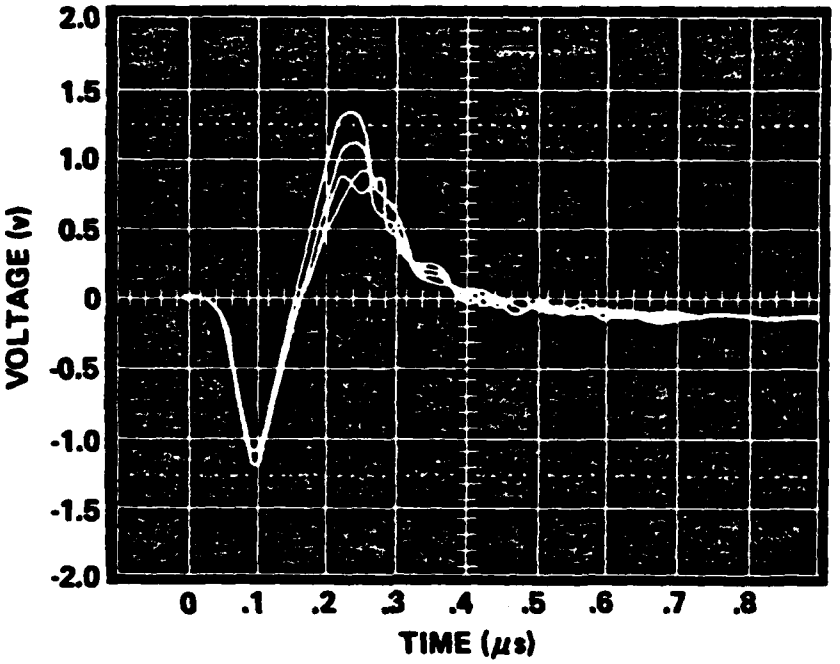

FIG. 30 1/2 mil Mylar Sample on Tank

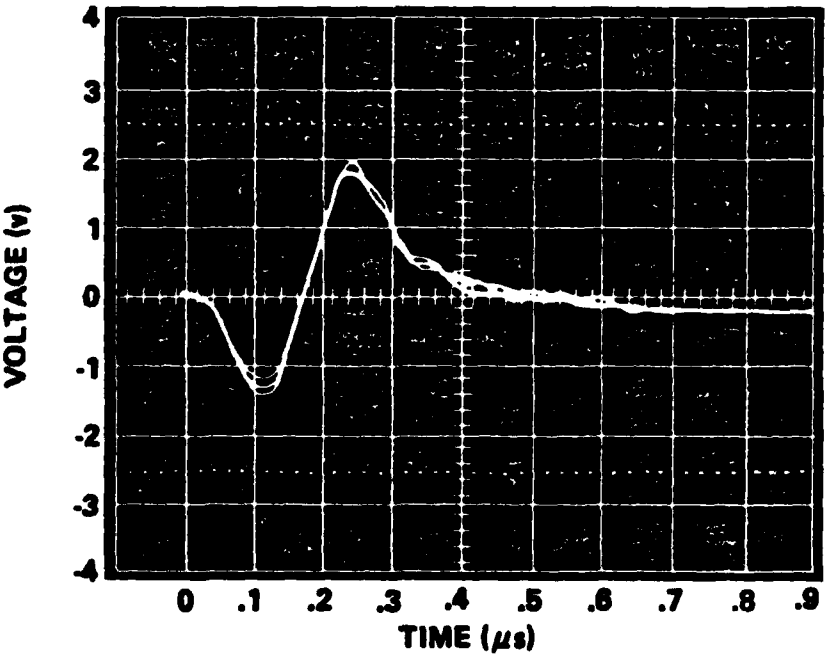

FIG. 31 2 mil Plus 1/2 mil Mylar Sample on Tank

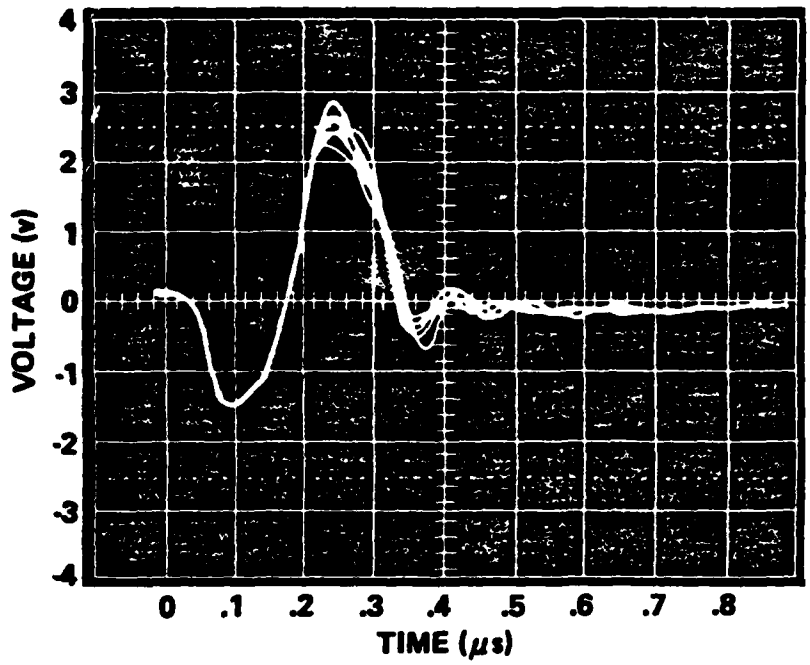

FIG. 32 3 mil Mylar Sample on Tank

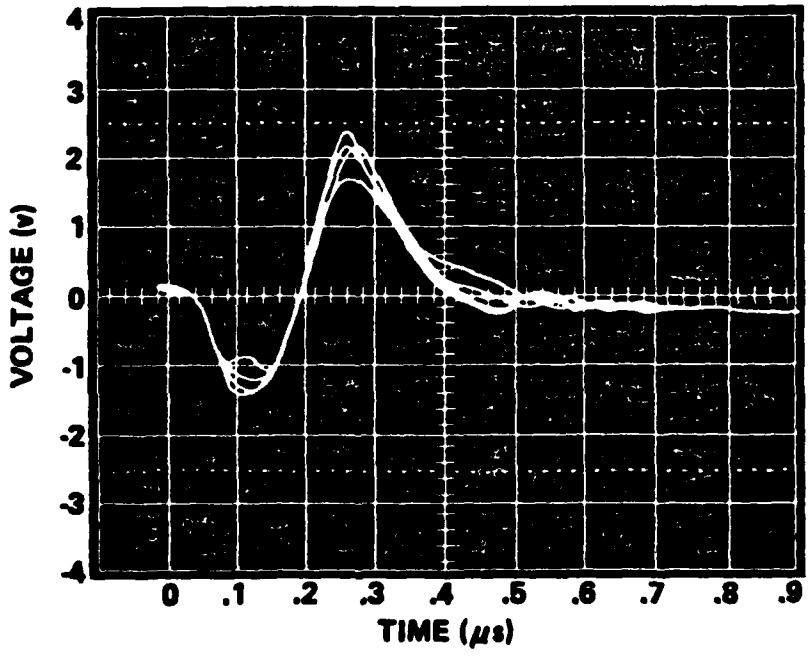

FIG. 33 4 mil Plus 1/2 mil Mylar Sample on Tank

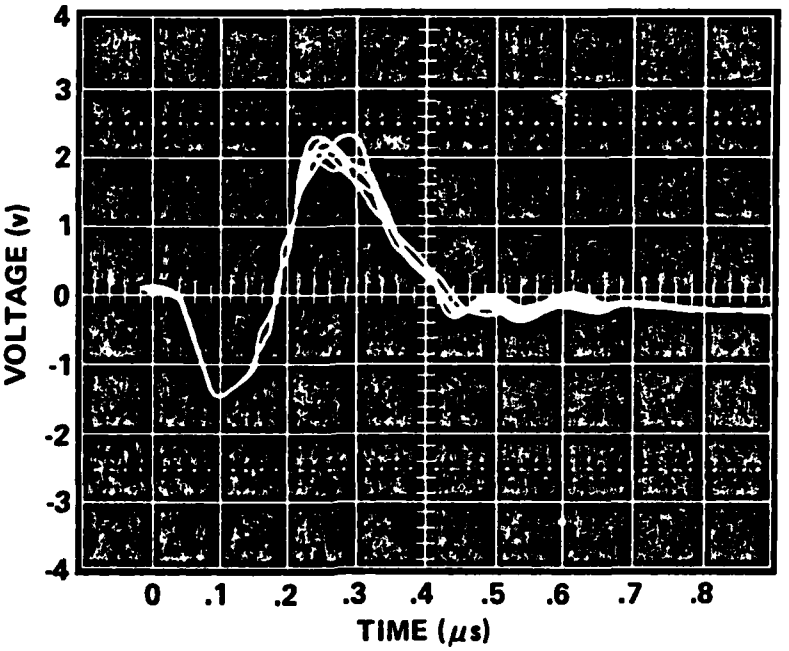

FIG. 34 5 mil Mylar Sample on Tank

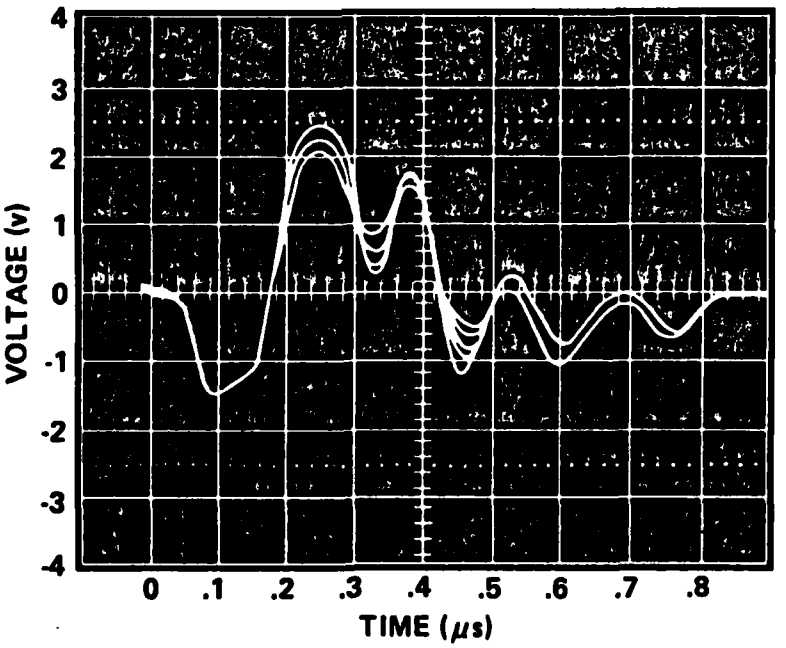

FIG. 35 7 mil Mylar Sample on Tank

5. TESTING, PHASE II

5.1 Introduction

In the second phase of testing the goal was to optimize the output. In these tests, samples were clamped in an opening made in the plastic side of the tank (Fig. 5). This was done so that the material could couple directly onto the water with no loss in the tank structure.

It was decided to continue the second phase of testing using two materials, Mylar and Teflon.

5.2 Beampatterns

A sample of 2 mil Teflon TFE was clamped over the opening in the tank and the tank was filled with water. As a comparison to the previous test, the output with the laser 6 inches away with an open aperture was recorded. A level of 4.5 v_{p-p} at 630 nsec was attained. This corresponds to 4.5 bars peak pressure in the tank. To determine whether ablation was contributing to the total output, tape was applied to the Teflon and the test rerun. The output was reduced to 2.5 v_{p-p} at the same frequency. This showed two things: that there is no ablation or other permanent physical changes occurring as a result of the laser radiation and that the tape does absorb some IR energy.

This test was rerun with a 3 mil Mylar sample. The full power laser beam also produced an output of 4.5 volts peak to peak at about 430 nsec, also corresponding to 9 bars peak to peak.

The tank was then moved onto the farfield, about 5 feet away, and the laser aperture closed to TEM_{00}. The output dropped to 1.0 v_{p-p} with these changes for both samples. The waveforms with the laser operating in a single mode were much more reproducible than with the laser operating in multimodes. The 1 v_{p-p} value

was used as a baseline for later focusing tests. Next, the beampattern for the Teflon sample was recorded. This was done by aligning the transducer with the center of the beam. Then, using the micrometer adjustments for lateral position, the response moving away from the center was recorded. This was done at several distances from the source and the results appear in Figs. 36 and 37. The vertical beampattern is supposed to be the same as the horizontal direction, due to the symmetrical nature of the source and the homogeneity of the medium. Vertical direction beampatterns could not be measured as there was no fine vertical adjustment. Output is also assumed to be symmetrical about the center axis in the horizontal plane. The beampattern for Mylar was not recorded.

These beampatterns are a function of both the sound beam and the directionality of the transducer. An omnidirectional sensor or the ability to accurately rotate the sensor are needed to produce the actual beampattern.

5.3 Design of a Zone Plate

The effectiveness of a zone plate in focusing the ultrasonic sound was investigated. A zone plate consists of a series of concentric rings. Each ring is at a distance of one wavelength further from the zone plate focus than is the previous ring. The radius of the n^{th} ring, r_n, is given by

$$r_n^2 = 2n \lambda F$$

where λ is the wavelength and F is the focal length. This is based on the well known theorem for the intersection of two chords of a circle. For the sound to be focused at a distance of 30 mm in water, the radius of each ring is $3 \sqrt{n}$ mm.

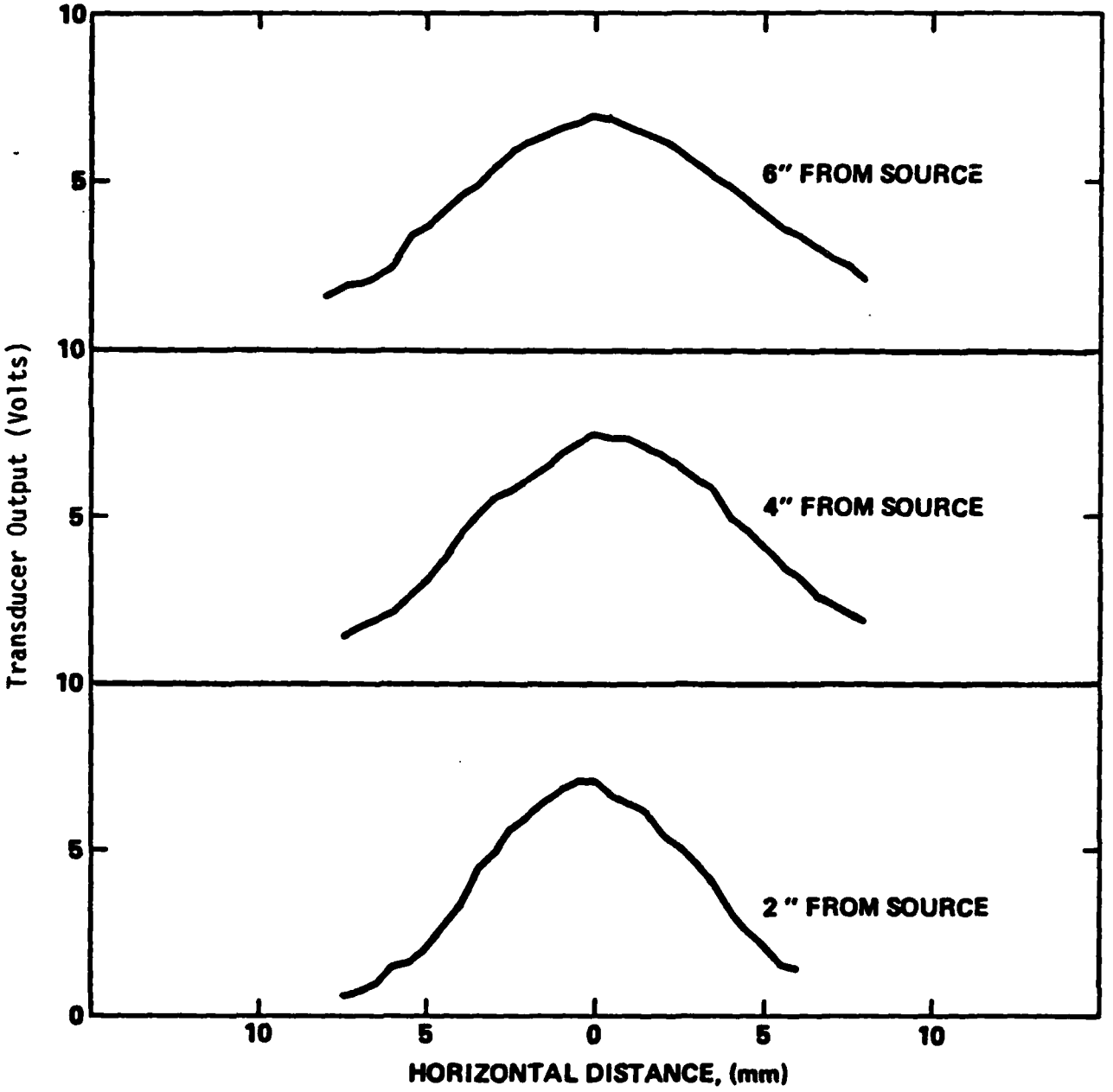

FIG. 36 Beampattern for 2 Mil Teflon Sample in Window

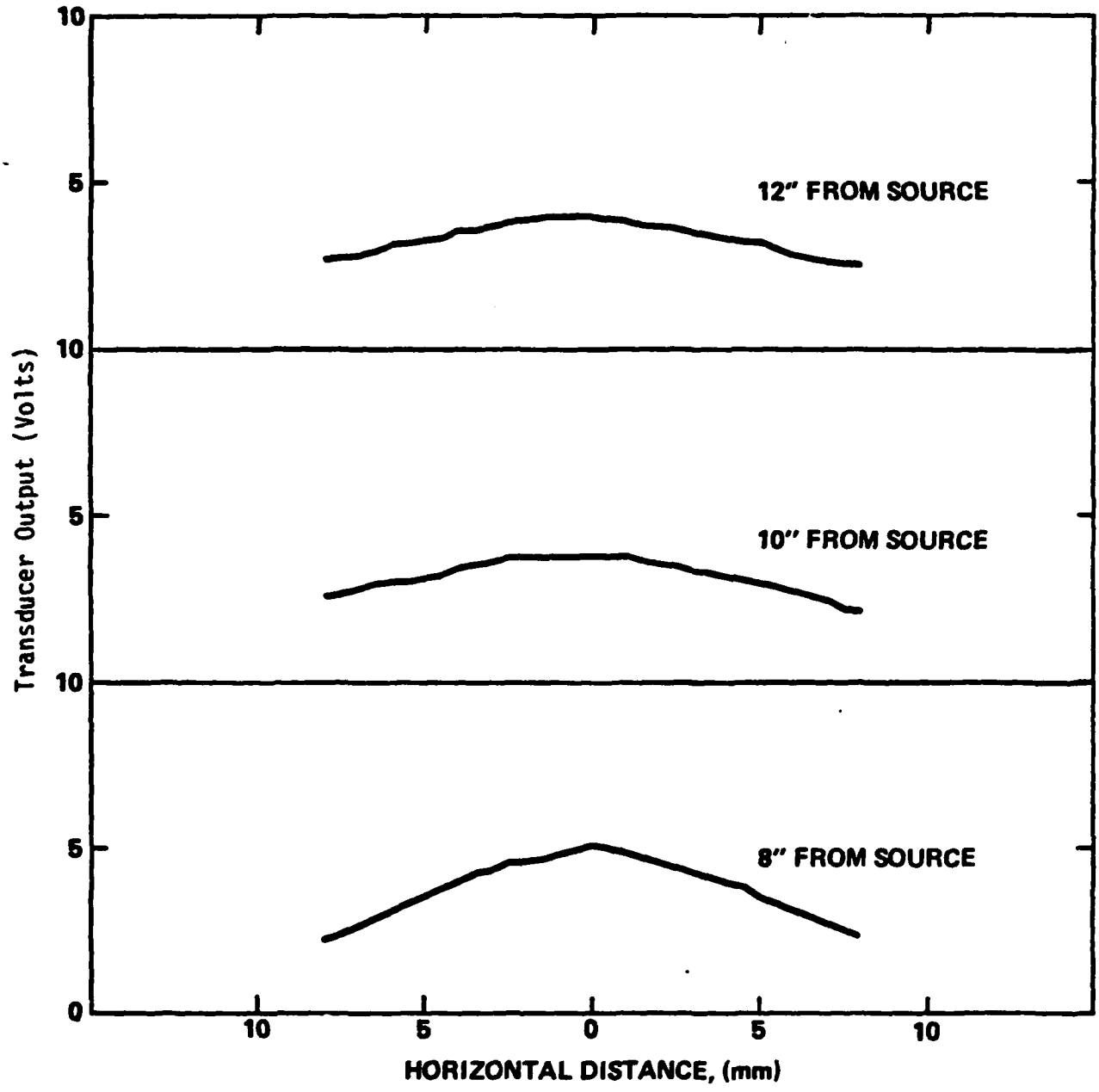

FIG. 37 Beampattern for 2 Mil Teflon Sample in Window

Now the only way we can make the zone plate is with an equal area of dark and light rings. Thus if 3 $\sqrt{n}$ is the outer radius of the ring 3 $\sqrt{n-1}$ is the inner radius of the ring. Thus in order to draw a zone plate, we draw a number of concentric rings with radii proportional to $\sqrt{n}$. We then block in every other ring.

To make an off-axis zone plate, a section of the rings, offset from their center, is used.

5.4 Focusing

The next step in testing was to determine whether the sound field could be focused, increasing its intensity at a given point. This was done with a holographic lens which consisted of an off-axis zone plate. The zone plate was supplied by NADC. It was generated by using a computer to draw the lines and from this drawing a grating was etched in molybdenum. (See Fig. 38.)

The zone plate received from NADC had a focal length of 3 cm at an angle of 45° and acoustic frequency of 10 MHz. It was taped to the surface of the target and the laser beam directed at it. For these tests, 4 different targets were tested. 3 mil Mylar, the 2 mil Teflon TFE (cloudy), and 1/2 mil Mylar were tested (expected to be similar to the Teflon). Also a 2 mil sample of Teflon FEP, a clear Teflon, was tested to see if any differences between the cloudy and clear samples existed.

With the 2 mil Teflon TFE sample, three beams were found. The first, or zero order, was very similar to the unfocused beam (Fig. 39) that appeared directly on axis, and was measured on a line 30 mm behind the target. The second was located 55° off axis to the focal side (Fig. 40) and the third located at about

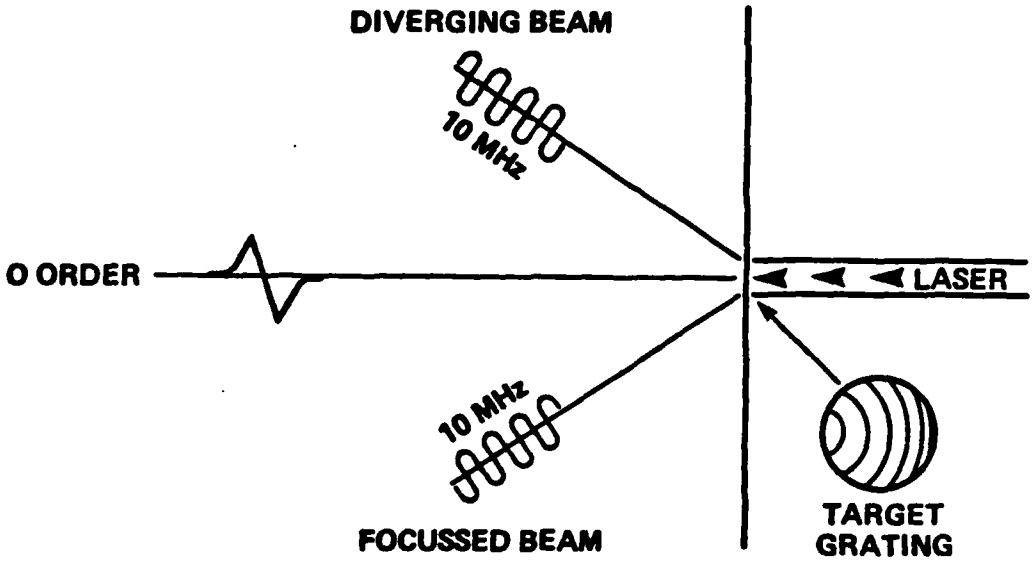

FIG. 38 Effect of Diffraction Grating on Image

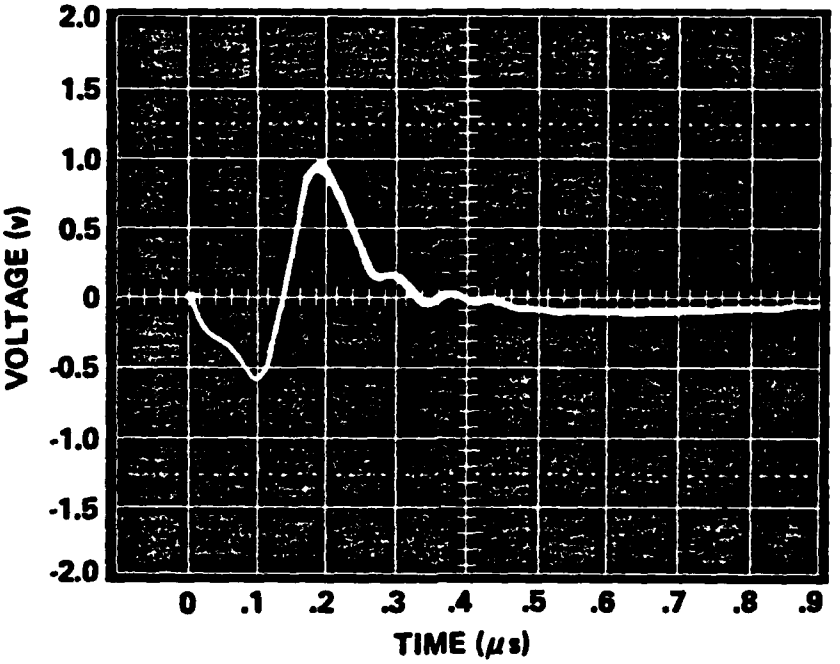

FIG. 39 2 mil Teflon TFE Target With Zone Plate

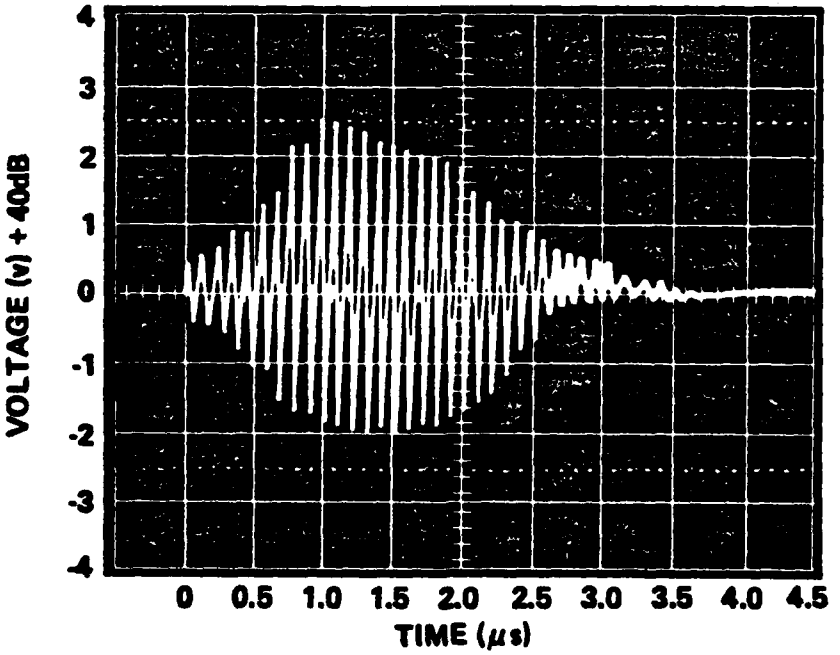

FIG. 40 2 mil Teflon TFE Target With Zone Plate, 55° Off Axis on Side of Focus

the same place on the side opposite to the focus (Fig. 41). The off-axis beams are the ones produced by diffraction by the zone plate. Instead of being an N wave, as the zero order is, these diffracted beams are envelopes of 10 MHz sine waves. One of the beams is presumed to be converging and the other is diverging. It is noted that these signals are about 30 dB less than the zero order beam. Due to the finite size of the measuring transducer (6 mm dia.) and the small beam diameter (1 cm) the actual focus could not be identified.

The 3 mil Mylar produced different results. The zero order beam was similar to the zero order beam noted from the Teflon, (Fig. 42). The only other beam noted was a low level, poorly focused image about 45° off axis, on the diverging side of the zone plate (Fig. 43). It was noted that the component frequency is slightly higher than that of the Teflon sample.

The clear FEP sample produced beams almost exactly like the cloudy TFE sample. These are pictured in Figs. 44 through 46. There was very little difference between the cloudy and clear samples. Lastly, the 1/2 mil Mylar sample was tested. It produced images similar to and slightly greater in magnitude than the Teflon samples (see Fig. 47 through 49). This is consistent with the thin Mylar and the Teflon samples absorbing very little of the incident beam and the absorption occurring in the water. It should also be noted that 7 mil Mylar was tested and produced no diffracted beam at all.

In all of these experiments only one diffracted beam was produced on each side, even though the excitation was a broadband pulse. The exact reason for this is not clear. For a given set of rings, the focal length is inversely proportional to the wavelength of the sound (page 42). Thus we would expect different focal lengths at different acoustic frequencies if

the target was excited with a broadband impulse. Further, because we are using an off-axis zone plate, these tones will be at different angles. However, instead, what we see is only a single monotonic tone burst at 45°. Further, the tone burst is 4 μsec long, whereas the laser pulse is only 50 nsec long. The 4 μsec does correspond to the range in transit times to be expected from across the target. For example, if the target were illuminated over a 10 mm diameter, then the range of arrival times is .01 sin 45°/c where c = 1,500 m/sec, the speed of sound in water. This time is 4.7 μsec. Therefore the duration of the tone burst is not unexpected.

However, it is still unexpected that the signal occurs at only one frequency, 10 MHz. One suggestion is that there are transverse flexural or Rayleigh waves induced in the target material. If these waves have a velocity of 2,000 m/sec for a frequency of 10 MHz, then there will be coincidence between the wavenumber of these waves and the sound waves. This wavenumber matching will greatly enhance the energy induced in the sound field. Calculations on these waves have not yet been performed.

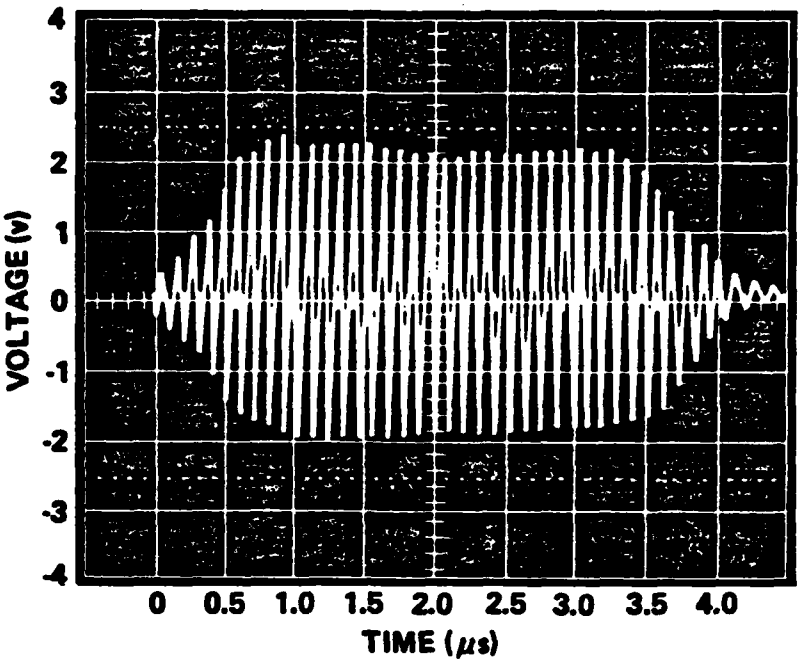

FIG. 41 2 mil Teflon TFE Target 60° Off Axis, Opposite Side From Focus

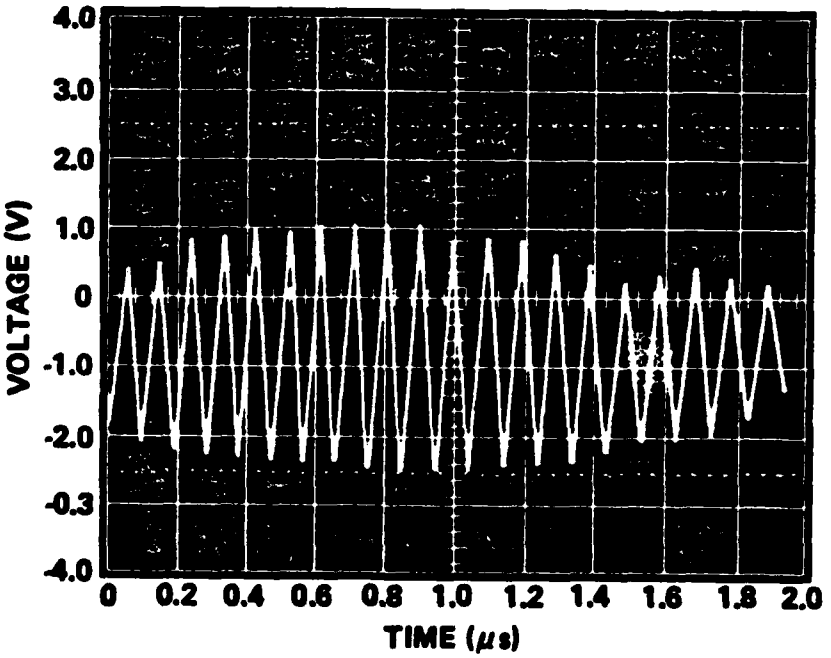

FIG. 41a Time Expanded Trace of Fig. 41

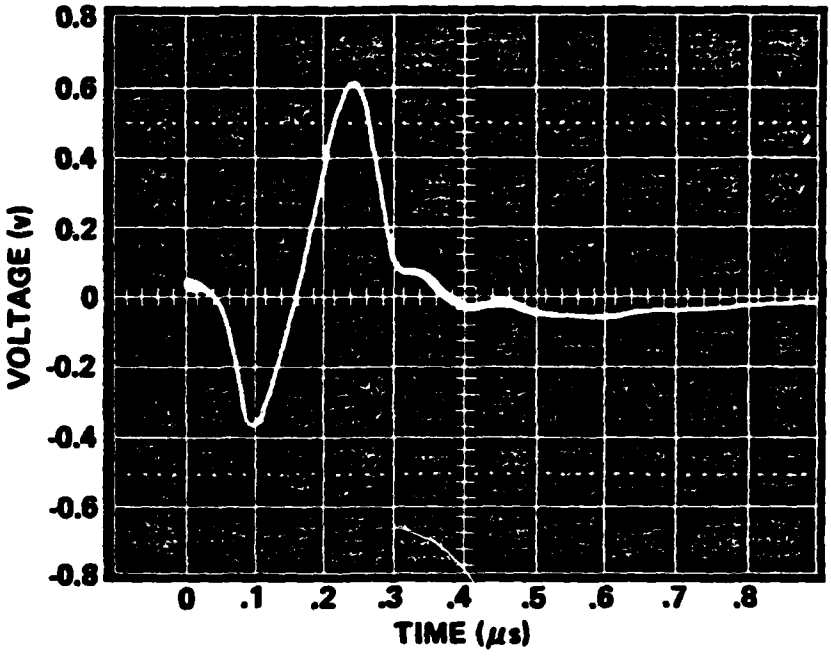

FIG. 42 3 mil Mylar Target With Zone Plate, Zero Order Beam

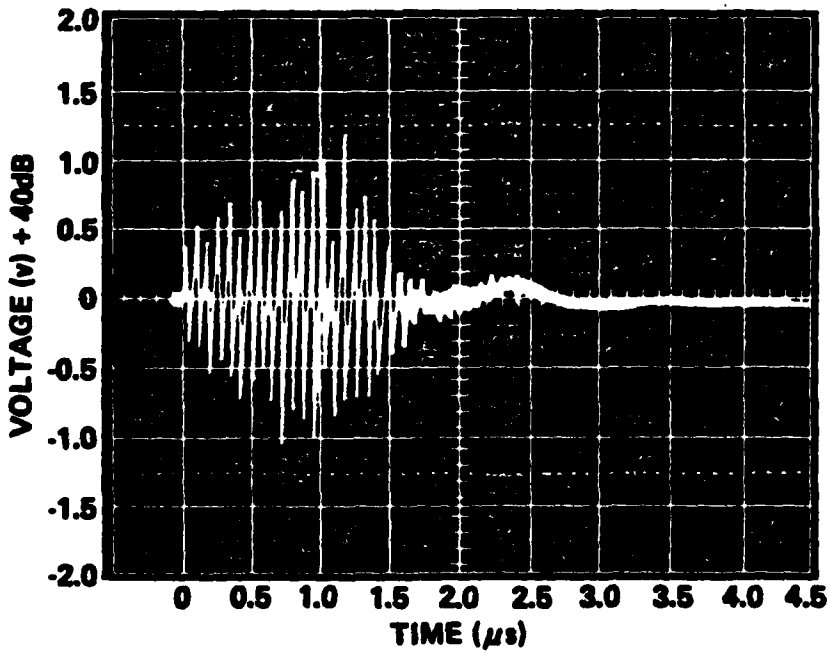

FIG. 43 3 mil Mylar Target With Zone Plate, 45° Off Axis, Opposite Focal Side

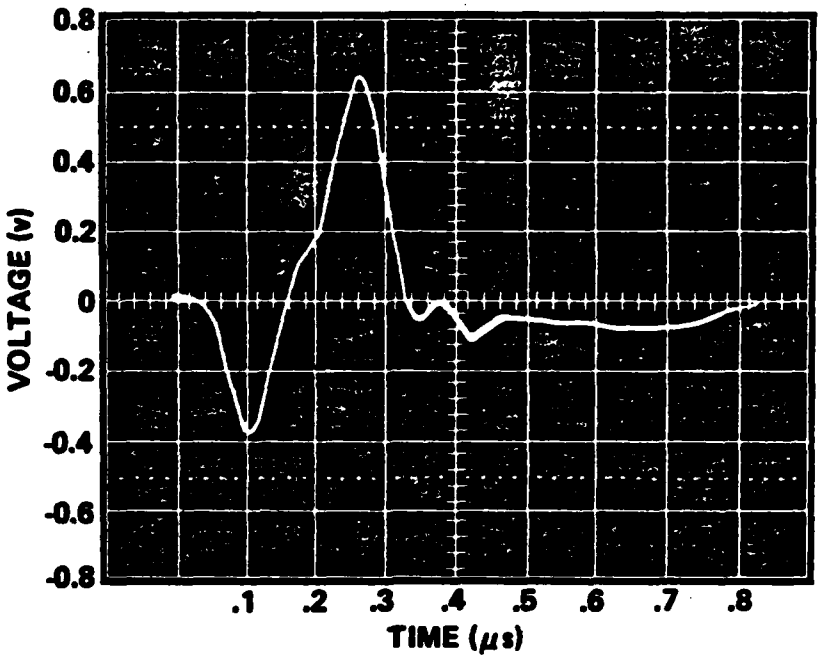

FIG. 44 2 mil Teflon FEP Target With Zone Plate, Zero Order Beam

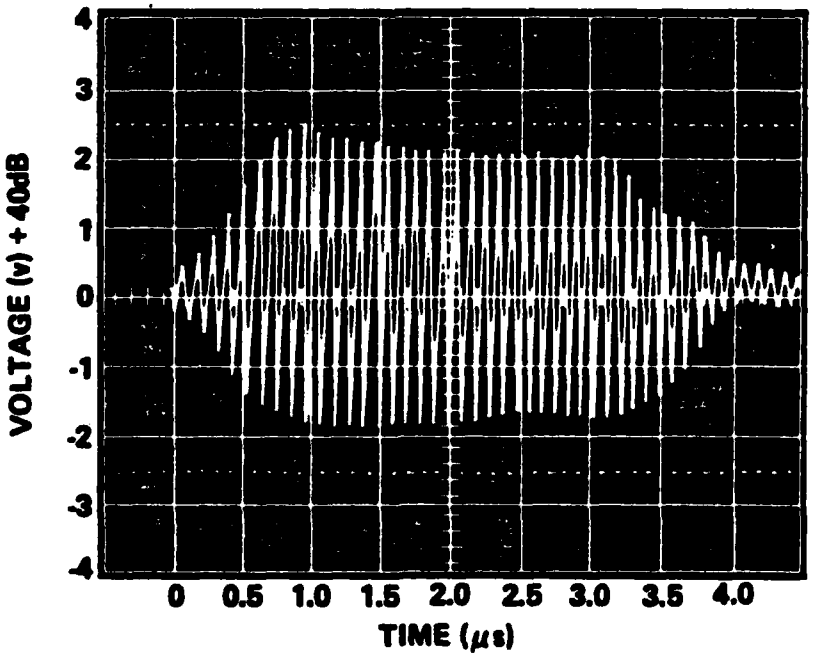

FIG. 45 2 mil Teflon FEP Target With Zone Plate, 60° Off Axis, Focal Side

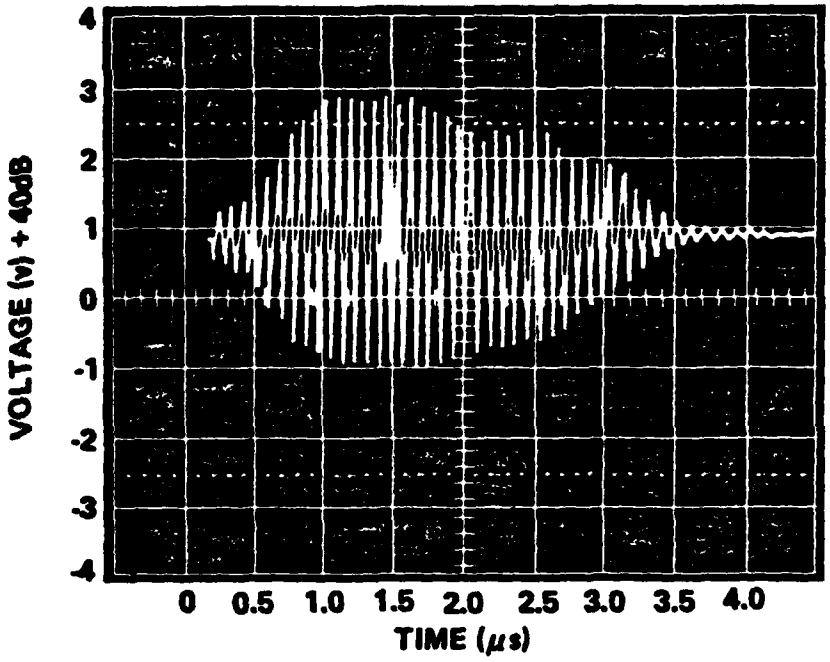

FIG. 46 2 mil Teflon FEP Target With Zone Plate, 50° Off Axis, Opposite Side to Focus

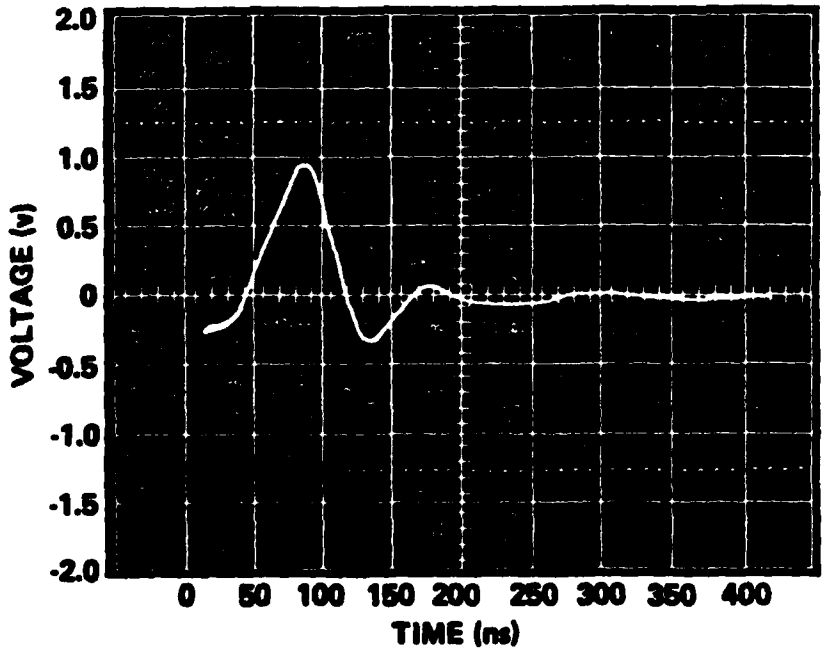

FIG. 47 1/2 mil Mylar Target With Zone Plate, Zero Order Beam

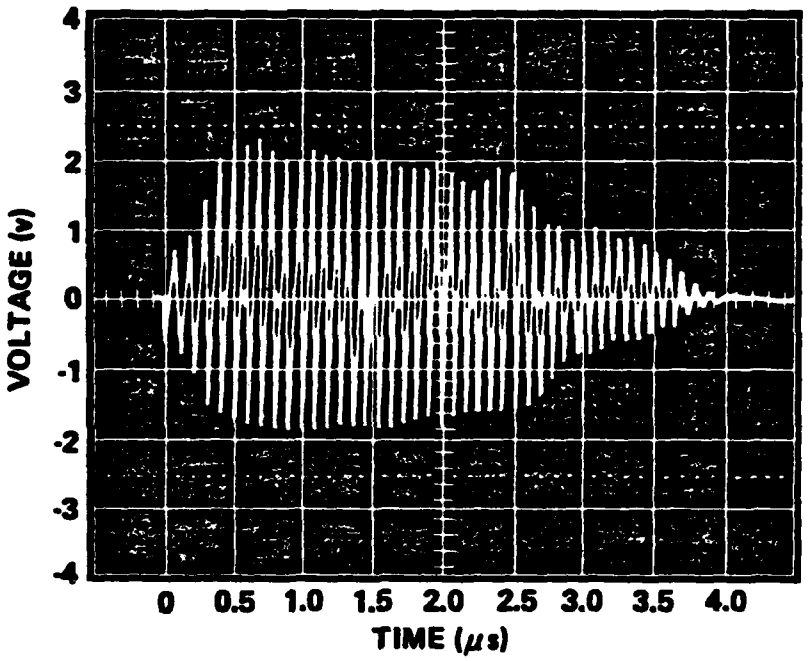

FIG. 48 1/2 mil Mylar Target With Zone Plate
50° Off Axis, Focal Side

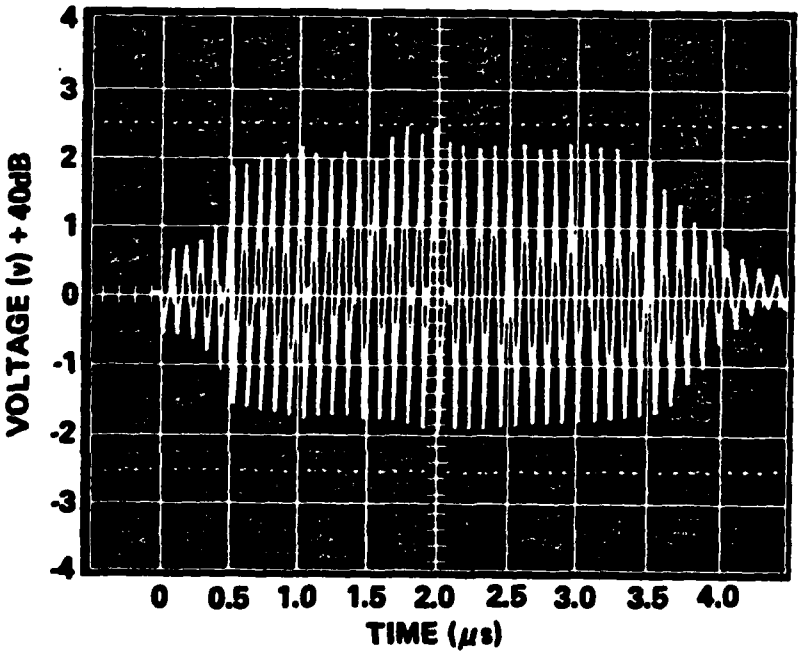

FIG. 49 1/2 mil Mylar Target With Zone Plate
60° Off Axis, Side Opposite Focus

5.5 Infra-red Absorption by Teflon and Mylar

The absorption of Teflon FEP and Mylar samples were measured in infra-red spectrometers and the spectra are shown in Figs. 50 and 51. A 50 μm sample of Teflon FEP was tested in a Perkin Elmer 137 infra-red spectrophotometer. At a wavelength of 10.6 μm, the transmission was 54% giving an absorption length of 82 μm.

The 75 μm Mylar sample was tested in a Fourier transform infra-red spectrophotometer. At a wavelength of 10.6 the transmission of the sample was 47%, giving an absorption length of 102 μm.

Thus both of these plastics have comparable absorption lengths which are both about 10 times that of water which is 10 μm.

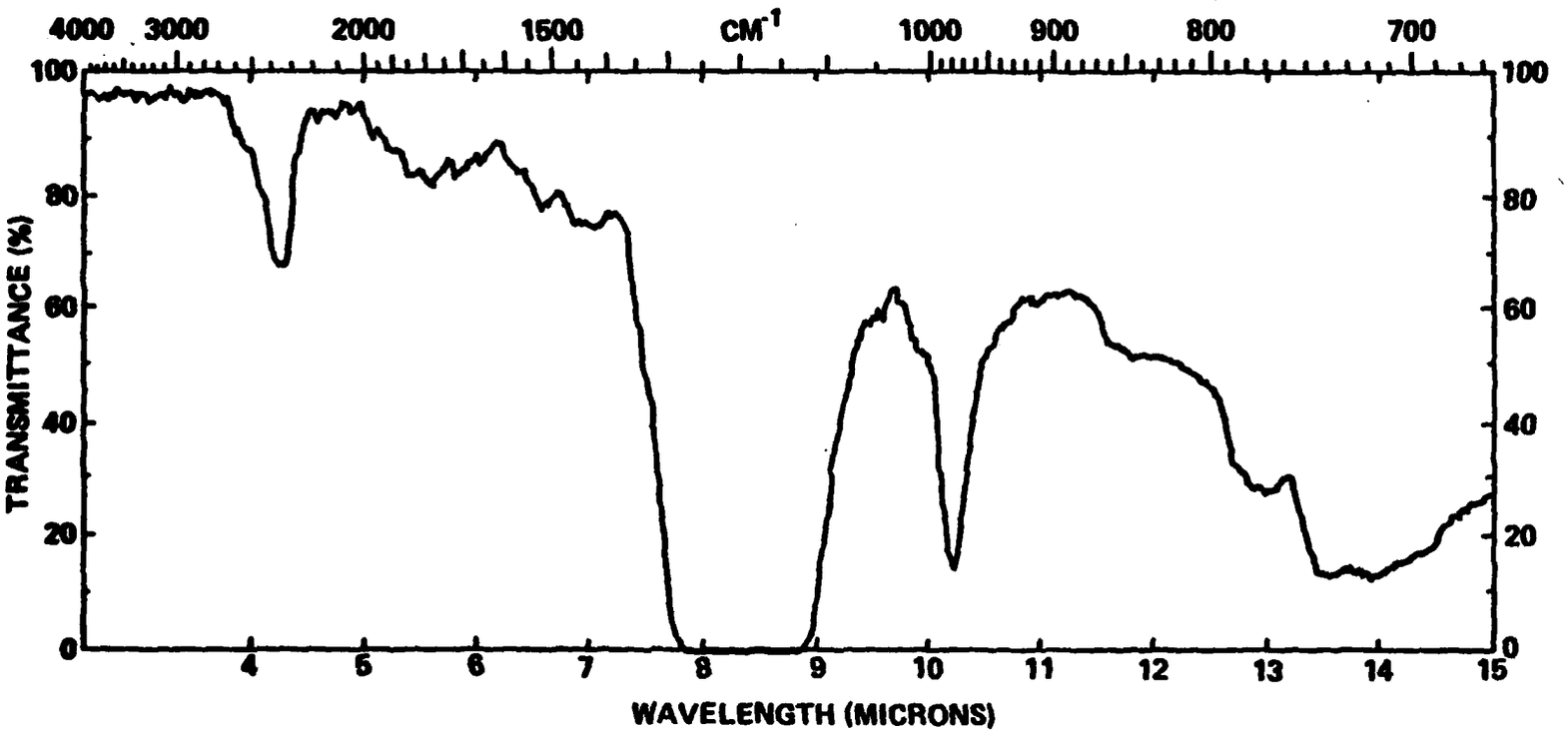

FIG. 50 IR Transmittance Spectrum for 3 Mil Mylar

FIG. 51 IR Transmittance Spectrum For 3 mil Mylar

6. SURFACE DAMAGE

When a laser pulse with a power density of 10^{11} watts/m^2 is fired at a surface, there is a very real question of surface damage. Indeed when the laser was fired at an aluminum surface, even one shot produced visible scratching of the surface. Further, when the laser was fired at a glass surface, about 50 shots produced severe crazing in the glass. However, when the laser was fired into most plastics, very little or no damage occurred. This is thought to be because the absorption coefficient is much less than for metals or glass and hence the absorption occurs in a much greater volume. This means that the maximum temperature reached is much lower.

During both phases of testing, only the Delrin plastic showed any surface damage when the laser was fired. The Delrin produced a loud cracking noise, accompanied by occasional flame and surface damage. To determine the ablative effects on this as well as other samples, "Scotch" tape was placed over the samples. The tape is predominantly polyethylene which transmits much of the radiation to the sample and yet restricts the release of the ablated gases. Thus, if ablation occurs, the tape should increase the intensity of the acoustic wave over the duration of the laser pulse.

For the Delrin sample, the output increased from .4 volts to 2 volts, confirming that significant ablation was occurring in the material. When the Teflon sample was tested in this manner, a decrease in signal was noted. This implies that the main mechanism with Teflon is not ablative. It was also noted that the repeatability of the Delrin sample was very poor (see page 16).

The 2 and 4 mil Mylar samples melted after 20 to 30 shots. The samples of Mylar supplied may have been different grades of Mylar. Covering these samples with additional 1/2 mil layers of a different grade of Mylar reduced the problem enough to make measurements possible. No ablation was noted.

With Teflon, the material withstood 100 pulses of 1 joule each over a period of 2 minutes without any damage, although the material did become quite hot to touch.

7. CONCLUSIONS

A laser can be used to generate ultrasonic pulses which are at least as intense as those generated with a conventional piezoceramic transducer. The waveform is typically an 'N' wave, 200 to 500 nseconds in duration and the peak pressure is of the order of 10 bars. When the laser was operated in a single (TEM_{00}) mode the results were extremely reproducible. However, this was not the case when the laser was operated in multi-modes.

The most efficient materials for this transduction were a wide variety of plastics, particularly Teflon and Mylar, which had relatively weak absorption of the infrared radiation. Metals and glass were relatively ineffective. Further, most of the plastics showed no damage from the laser pulses, whereas metals were schorched and glass crazed. This is thought to be due to the relatively large depth over which the energy is absorbed in the plastics.

A holographic lens, or zone plate, was used to generate a diffracted beam. The lens was designed to give a focus 45° off axis at a frequency of 10 MHz and this is what was found. The waveform was a 10 MHz tone burst rather than an 'N' wave as measured in the zero order beam. Beams were found on both sides of the zone plate. No other beams or any other frequencies were found.

A theory of the thermoelastic wave generation process has been presented and this gives good agreement both qualitatively in terms of the waveform measured and quantitatively in terms of the peak pressures and durations of the waveforms which were measured.

Further work needs to be undertaken on understanding the mechanisms in the different plastics. A thin, almost transparent, plastic is almost as effective as a thicker opaque sample. Techniques for generating different waveforms using different grating patterns should be investigated further.

So far all measurements have concerned the generation of ultrasound in water. Further work should be undertaken to study the generation in metals. Since there is a bigger impedance mismatch between plastics and water, plastics may not be the optimum target materials. Further sheer waves can be generated in metals, which they cannot in water, and these may prove to be much more useful than longitudinal waves.

Finally, further studies should be made into coincidence effects between the speeds of flexural or Rayleigh waves in the target materials and the speeds of propagating waves in the test material. Considerable enhancement will occur if we can make use of these coincidence effects.

REFERENCES

R.J. VonGutfeld (1980), "Laser Generated Elastic Waves for Ultrasonic Generation," Naval Air Development Center Report No. NADC-28240-60.

G.D. Hickman, B.S. Maccabee and C.E. Bell (1980a), "Feasibility Study of Airborne Bathymetric Sensing Using the CO_2 Laser/Acoustic Technique," Office of Naval Research Report No. AST-R-070580.

B.S. Maccabee, C.E. Bell and G.D. Hickman (1980b), "Beneath and Above Water Echo Detection Using a Laser Induced Sound Source," Report on NAVAIR Task A035370K/009B/OF-371-000.

C.E. Bell and B.S. Maccabee (1974), "Shock Wave Generation in Air and in Water by CO_2 TEA Laser Radiation Applied Optics," Vol. 13, pp. 605-609.

J.P. Reilly, A. Ballantine, and J.A. Woodroffe (1979), "Modeling of Momentum Transfer to a Surface by Laser-Supported Absorption Waves," AIAA Journal Vol. 17, pp. 1098-1105.

L.E. Kinder and A.R. Frey (1962), *Fundamentals of Acoustics* Wiley and Sons, New York.

L.L. Beranek (1954), *Acoustics*, McGraw-Hill, New York.

DISTRIBUTION LIST

REPORT NO. NADC-81067-60

	No. of Copies
NAVAIR (AIR-004D) (2 for retention) (1 for AIR-320) (1 for AIR-4114C) (1 for AIR-5163) (1 for AIR-5163B) (1 for AIR-51632) (1 for AIR-51632D)	8
WPAFB, OH (AFWAL-LLP/MLLP) (Dr. Robert Crane)	1
NAVSHIPRSCHDEVCEN, Annapolis, MD (Code 2823)	1
NAVSWC, Silver Spring, MD (J. F. Goff, C. Anderson)	2
NRL, Washington, DC (I. Wolock, H. Chaskelis, Dr. C. Sanday)	3
NAVAIRENGCEN, Lakehurst, NJ (D. Behmke, Code 92713, P. Ciekurs, Code 92724)	2
NAVSEA, Washington, DC (Dr. H. Vanderveldt, Code OR15)	1
DARPA, Arlington, VA (CAPT S. Wax)	1
ONR, Arlington, VA (Dr. Y. Rajapakse, Code 432)	1
NASA, Langley, Hampton, VA (Dr. J. Heyman)	1
NASA, Lewis Research Center, Cleveland, OH (A. Vary)	1
AMMRC, Watertown, MA (G. Darcy, R. Brockelman)	2
IBM Watson Research Center, Yorktown Heights, NY (R. J. von Gutfeld)	1
Lockheed Missiles & Space Company, Inc., Sunnyvale, CA (Dr. M. I. Jacobson)	1
University of Delaware, Newark, DE (Dr. R. B. Pipes, R. Blake)	2
Lawrence Livermore Laboratories, Livermore, CA (Dr. S. J. Kulkarni, Code L502)	1
Johns Hopkins University, Baltimore, MD (Dr. R. Green, Jr.)	1
Ames Laboratory, Energy & Mineral Resources Research Institute (Dr. D. Thompson)	1
DTIC	12

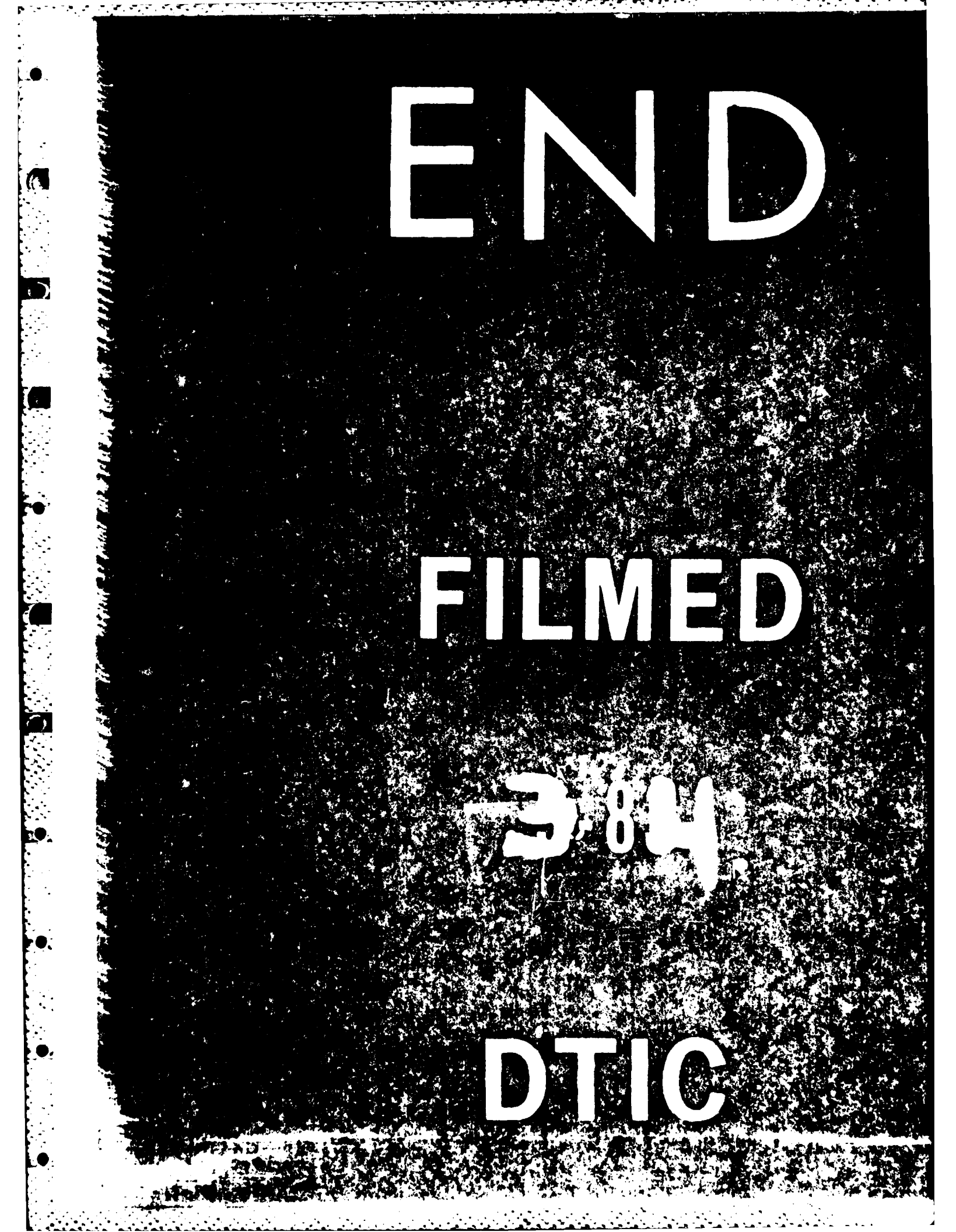
END
FILMED
3-84
DTIC